proliferation in wild-type mice [27]. We therefore hypothesised that both glucose metabolism and Ca^{2+} influx are required to increase *Irs2* expression and lead to beta cell proliferation. This hypothesis is supported by a report that glibenclamide increases beta cell proliferation in the presence of an increased glucose flux [27].

The *Pdx1* expression level has been reported to be severely reduced in the beta cells of *Irs2*$^{-/-}$ mice with a certain genetic background [28], suggesting that IRS2 may directly regulate the expression and function of *Pdx1*, and thereby maintain beta cell growth and function. However, GKA upregulated the expression of *Pdx1* and several downstream genes, *Glut2*, *Gck*, *Ins1* and *Ins2*, in the isolated islets of *Irs2*$^{-/-}$ mice with a C57BL/6 background (Fig. 4b). In regard to this point, Suzuki et al reported finding that *Pdx1* expression in *Irs2*$^{-/-}$ mice is regulated in a strain-dependent manner [29]. *Pdx1* expression was not downregulated in our *Irs2*$^{-/-}$ murine beta cells that had a C57BL/6J background [29]. We therefore assume that GKA increased glucose-stimulated insulin gene transcription independently of IRS2. Since Kushner et al reported that transgenic overexpression of *Pdx1* restored beta cell mass in *Irs2*$^{-/-}$ mice [28], *Pdx1* may play a role in regulating beta cell mass. Nevertheless, because a haploinsufficiency of *Pdx1* led to impaired beta cell function, but not to decreased beta cell mass [30], and because beta cell mass was smaller in our *Irs2*$^{-/-}$ mice than in wild-type mice despite the *Pdx1* expression level being maintained [29], two different pathways are involved in the stimulation of beta cell function and proliferation by a GKA.

The results of our study have clinical implications. As stated above, MK-0941 lacked durability in glycaemic control [20]. In these patients, disease-related characteristics were a mean baseline HbA_{1c} of 9.0 % (75 mmol/mol), a mean duration of diabetes of 12 years, and a mean insulin glargine (A21Gly,B31Arg,B32Arg human insulin) dose of 45 U/day. These data suggest that the insulin secretion or the beta cells themselves were severely impaired. From these clinical trials, it is possible that a pancreatic effect of GKAs could not be expected when pancreatic beta cells have been impaired. It is well known that the level of 8-hydroxydeoxyguanosine, a marker of oxidative stress, is increased in diabetic patients and independently associated with mean HbA_{1c} [31]; in addition, increased oxidative stress influences beta cell function, and antioxidant treatment can exert beneficial effects in diabetes, with a preservation of beta cell function [32]. We therefore investigated the effect of oxidative stress on GKA-induced changes in the expression of genes involved in beta cell function and proliferation. As expected, the results showed that oxidative stress inhibited the upregulation of *Irs2* and *Pdx1* in response to GKA, although the inhibition was prevented by prior administration of an antioxidant (Fig. 5). Moreover, the levels of these molecules were not increased by GKA in islets isolated from *db/db* mice (Fig. 6).

Although our findings could support the observation that GKA is ineffective in patients with type 2 diabetes whose pancreatic beta cells have been impaired, there are some limitations to our study. First, with regard to the experiment with exogenous H_2O_2, we could not rule out the possibility that the absence of increasing *Irs2* and *Pdx1* expression after H_2O_2 preconditioning was caused by not only impaired mitochondrial function, but also an impaired biological response of these islets independently of GKA activity. It is also possible that *Gck* expression level might have an effect on the inhibition of upregulation of *Irs2* and *Pdx1* induced by 5.6 mmol/l glucose plus GKA. Second, with regard to the experiment with the *db/db* mice, GKA compounds act to reduce glucose levels in the *db/db* mouse model, as shown with MK-0941 and other agents [8, 33]. The background of the *db/db* mice or the difference in compounds could influence the effect of GKAs. Thus, greater study of the glucose-lowering effect of the GKA in *db/db* mice is needed.

In the present study, we also explored the therapeutic strategy by which GKA worked more effectively in these impaired beta cells. Based on the results of this study, we propose that GKA should be used before pancreatic beta cell failure. First, GKA should be used earlier, as diabetes is progressing, since beta cell failure has already progressed before the diagnosis of diabetes is made [34, 35]. The efficacy of long-term GKA therapy should be assessed in patients with mild type 2 diabetes or impaired glucose tolerance. Second, GKA should be used in combination with incretin therapy in case GKA monotherapy is ineffective. The results of our study indicated that GKA stimulated *Irs2* and *Pdx1* expression in the islets of *db/db* mice when exendin-4 had been administered in advance (Fig. 7). This finding suggested that combination therapy consisting of a GKA and an incretin may be useful for patients with type 2 diabetes. We previously speculated that the increase in *Irs2* expression in the islets of *db/db* mice in response to the combination of these drugs was due to the reduction of oxidative stress or the additive effect of Ca^{2+} influx via glucose signalling and cAMP signalling through the human glucagon-like peptide-1 receptors [22]. However, the levels of expression of the genes for the reduced-form NADPH oxidase complex were unchanged by prior administration of exendin-4 under our experimental conditions (Fig. 7e–g). Since *Irs2* expression was not increased by exendin-4 alone (Fig. 7c), we assume that exendin-4 amplifies GKA-stimulated calcium signalling rather than imposing it. Further study is needed to test the combination in vivo on glycaemic control and the resultant changes in pancreatic gene transcription.

In conclusion, GKA-stimulated IRS2 production affected beta cell proliferation, but not beta cell function. Oxidative

stress was able to prohibit the ability of GKA to change the expression of genes involved in beta cell function and proliferation. A combination of GKA and an incretin-related agent might be effective here. These findings suggest that the GKAs should have outstanding potential for the treatment of diabetes and related disorders.

Acknowledgements We thank M. Kaji and E. Sakamoto (Yokohama City University, Yokohama, Japan) for their excellent technical assistance and animal care.

Funding This work was supported in part by a Grant-in-Aid for Scientific Research (B) 19390251 and (B) 21390282 from the Ministry of Education, Culture, Sports, Science and Technology (MEXT) of Japan, a Medical Award from the Japan Medical Association, a Grant-in-Aid from the Japan Diabetes Foundation, a Grant-in-Aid from Novo Nordisk Pharma, a Grant-in-Aid from the Suzuken Memorial Foundation, a Grant-in-Aid from the Naito Foundation, a Grant-in-Aid from the Yamaguchi Endocrine Research Foundation, a Grant-in-Aid from the Uehara Memorial Foundation (to Y. Terauchi) as well as a Grant-in-Aid for Young Scientists (Start-up) 21890213 and (B) 23791040 from the MEXT of Japan, a Grant-in-Aid from Yokohama General Promotion Foundation, and a Grant-in-Aid from Japan Diabetes Foundation (to A. Nakamura).

Duality of interest The authors declare that there is no duality of interest associated with this manuscript.

Contribution statement All authors conceived and designed the study, and participated in the analysis and interpretation of the data. AN drafted the manuscript and all other authors revised it critically for intellectual content. All authors approved the final version of the paper.

References

1. Matschinsky FM (1996) Banting Lecture 1995. A lesson in metabolic regulation inspired by the glucokinase glucose sensor paradigm. Diabetes 45:223–241
2. Matschinsky FM, Glaser B, Magnuson MA (1998) Pancreatic beta-cell glucokinase: closing the gap between theoretical concepts and experimental realities. Diabetes 47:307–315
3. Terauchi Y, Takamoto I, Kubota N et al (2007) Glucokinase and IRS-2 are required for compensatory beta cell hyperplasia in response to high-fat diet-induced insulin resistance. J Clin Invest 117:246–257
4. Kassem S, Bhandari S, Rodríguez-Bada P et al (2010) Large islets, beta-cell proliferation, and a glucokinase mutation. N Engl J Med 362:1348–1350
5. Grimsby J, Sarabu R, Corbett WL et al (2003) Allosteric activators of glucokinase: potential role in diabetes therapy. Science 301:370–373
6. Efanov AM, Barrett DG, Brenner MB et al (2005) A novel glucokinase activator modulates pancreatic islet and hepatocyte function. Endocrinology 146:3696–3701
7. Futamura M, Hosaka H, Kadotani A et al (2006) An allosteric activator of glucokinase impairs the interaction of glucokinase and glucokinase regulatory protein and regulates glucose metabolism. J Biol Chem 281:37668–37674
8. Fyfe MC, White JR, Taylor A et al (2007) Glucokinase activator PSN-GK1 displays enhanced antihyperglycaemic and insulinotropic actions. Diabetologia 50:1277–1287
9. Coope GJ, Atkinson AM, Allott C et al (2006) Predictive blood glucose lowering efficacy by glucokinase activators in high fat fed female Zucker rats. Br J Pharmacol 149:328–335
10. Gorman T, Hope DC, Brownlie R et al (2008) Effect of high-fat diet on glucose homeostasis and gene expression in glucokinase knockout mice. Diabetes Obes Metab 10:885–897
11. Nakamura A, Terauchi Y, Ohyama S et al (2009) Impact of small molecule glucokinase activator on glucose metabolism, beta cell function and mass. Endocrinology 150:1147–1154
12. Nakamura A, Shimazaki H, Ohyama S, Eiki J, Terauchi Y (2011) Effect of long-term treatment with a small-molecule glucokinase activator on glucose metabolism, lipid profiles and hepatic function. J Diabetes Invest 2:276–279
13. Johnson D, Shepherd RM, Gill D, Gorman T, Smith DM, Dunne MJ (2007) Glucose-dependent modulation of insulin secretion and intracellular calcium ions by GKA50, a glucokinase activator. Diabetes 56:1694–1702
14. Wei P, Shi M, Barnum S, Cho H, Carlson T, Fraser JD (2009) Effects of glucokinase activators GKA50 and LY2121260 on proliferation and apoptosis in pancreatic INS-1 beta cells. Diabetologia 52:2142–2150
15. Withers DJ, Gutierrez JS, Towery H et al (1998) Disruption of IRS-2 causes type 2 diabetes in mice. Nature 391:900–904
16. Kubota N, Tobe K, Terauchi Y et al (2000) Disruption of insulin receptor substrate-2 causes type 2 diabetes due to liver insulin resistance and lack of compensatory beta-cell hyperplasia. Diabetes 49:1880–1889
17. Kubota N, Terauchi Y, Tobe K et al (2004) Insulin receptor substrate 2 plays a crucial role in beta cells and the hypothalamus. J Clin Invest 114:917–927
18. Matschinsky FM (2009) Assessing the potential of glucokinase activators in diabetes therapy. Nat Rev Drug Discov 8:399–416
19. Bonadonna RC, Heise T, Arbet-Engels C et al (2010) Piragliatin (RO4389620), a novel glucokinase activator, lowers plasma glucose both in the postabsorptive state and after a glucose challenge in patients with type 2 diabetes mellitus: a mechanistic study. J Clin Endocrinol Metab 95:5028–5036
20. Meininger GE, Scott R, Alba M et al (2011) Effects of MK-0941, a novel glucokinase activator, on glycemic control in insulin-treated patients with type 2 diabetes. Diabetes Care 34:2560–2566
21. Iino T, Hashimoto N, Sasaki K et al (2009) Structure-activity relationships of 3,5-disubstituted benzamides as glucokinase activators with potent in vivo efficacy. Bioorg Med Chem 17:3800–3809
22. Weir GC, Bonner-Weir S (2007) A dominant role for glucose in beta cell compensation of insulin resistance. J Clin Invest 117:81–83
23. Lingohr MK, Briaud I, Dickson LM et al (2006) Specific regulation of IRS-2 expression by glucose in rat primary pancreatic islet beta-cells. J Biol Chem 281:15884–15892
24. Maechler P, Jornot L, Wollheim CB (1999) Hydrogen peroxide alters mitochondrial activation and insulin secretion in pancreatic beta cells. J Biol Chem 274:27905–27913
25. Jhala US, Canettieri G, Screaton RA et al (2003) cAMP promotes pancreatic beta-cell survival via CREB-mediated induction of IRS2. Genes Dev 17:1575–1580
26. Ashcroft FM (2005) ATP-sensitive potassium channelopathies: focus on insulin secretion. J Clin Invest 115:2047–2058
27. Porat S, Weinberg-Corem N, Tornovsky-Babaey S et al (2011) Control of pancreatic beta cell regeneration by glucose metabolism. Cell Metab 13:440–449
28. Kushner JA, Ye J, Schubert M et al (2002) Pdx1 restores beta cell function in Irs2 knockout mice. J Clin Invest 109:1193–1201
29. Suzuki R, Tobe K, Terauchi Y et al (2003) Pdx1 expression in Irs2-deficient mouse beta-cells is regulated in a strain-dependent manner. J Biol Chem 278:43691–43698
30. Shih DQ, Heimesaat M, Kuwajima S, Stein R, Wright CV, Stoffel M (2002) Profound defects in pancreatic beta-cell function in mice

with combined heterozygous mutations in Pdx-1, Hnf-1α, and Hnf-3β. Proc Natl Acad Sci U S A 99:3818–3823
31. Nishikawa T, Sasahara T, Kiritoshi S et al (2003) Evaluation of urinary 8-hydroxydeoxy-guanosine as a novel biomarker of macrovascular complications in type 2 diabetes. Diabetes Care 26:1507–1512
32. Kaneto H, Kajimoto Y, Miyagawa J et al (1999) Beneficial effects of antioxidants in diabetes. Possible protection of pancreatic beta cells against glucose toxicity. Diabetes 48:2398–2406
33. Eiki J, Nagata Y, Futamura M et al (2011) Pharmacokinetic and pharmacodynamic properties of the glucokinase activator MK-0941 in rodent models of type 2 diabetes and healthy dogs. Mol Pharmacol 80:1156–1165
34. Kendall DM, Cuddihy RM, Bergenstal RM (2009) Clinical application of incretin-based therapy: therapeutic potential, patient selection and clinical use. Am J Med 122:S37–S50
35. Butler AE, Janson J, Bonner-Weir S, Ritzel R, Rizza RA, Butler PC (2003) Beta-cell deficit and increased beta-cell apoptosis in humans with type 2 diabetes. Diabetes 52:102–110

Effects of Liraglutide on β-Cell-Specific Glucokinase-Deficient Neonatal Mice

Jun Shirakawa, Ritsuko Tanami, Yu Togashi, Kazuki Tajima, Kazuki Orime, Naoto Kubota, Takashi Kadowaki, Yoshio Goshima, and Yasuo Terauchi

Departments of Endocrinology and Metabolism (J.S., R.T., Y.To., K.T., K.O., Y.Te.) and Molecular Pharmacology and Neurobiology (J.S., Y.G.), Graduate School of Medicine, Yokohama-City University, Yokohama 236-0004, Japan; and Department of Diabetes and Metabolic Diseases (N.K., T.K.), Graduate School of Medicine, University of Tokyo, Tokyo 113-0033, Japan

The glucagon-like peptide-1 receptor agonist liraglutide is used to treat diabetes. A hallmark of liraglutide is the glucose-dependent facilitation of insulin secretion from pancreatic β-cells. In β-cells, the glycolytic enzyme glucokinase plays a pivotal role as a glucose sensor. However, the role of glucokinase in the glucose-dependent action of liraglutide remains unknown. We first examined the effects of liraglutide on glucokinase haploinsufficient ($Gck^{+/-}$) mice. Single administration of liraglutide significantly improved glucose tolerance in $Gck^{+/-}$ mice without increase of insulin secretion. We also assessed the effects of liraglutide on the survival rates, metabolic parameters, and histology of liver or pancreas of β-cell-specific glucokinase-deficient ($Gck^{-/-}$) newborn mice. Liraglutide reduced the blood glucose levels in $Gck^{-/-}$ neonates but failed to prolong survival, and all the mice died within 1 wk. Furthermore, liraglutide did not improve glucose-induced insulin secretion in isolated islets from $Gck^{-/-}$ neonates. Liraglutide initially prevented increases in alanine aminotransferase, free fatty acids, and triglycerides in $Gck^{-/-}$ neonates but not at 4 d after birth. Liraglutide transiently prevented liver steatosis, with reduced triglyceride contents and elevated glycogen contents in $Gck^{-/-}$ neonate livers at 2 d after birth. Liraglutide also protected against reductions in β-cells in $Gck^{-/-}$ neonates at 4 d after birth. Taken together, β-cell glucokinase appears to be essential for liraglutide-mediated insulin secretion, but liraglutide may improve glycemic control, steatosis, and β-cell death in a glucokinase-independent fashion. (***Endocrinology* 153: 3066–3075, 2012**)

The incretin glucagon-like peptide-1 (GLP-1) facilitates glucose-stimulated insulin release and contributes to plasma glucose homeostasis (1, 2). GLP-1 receptor (GLP1R) agonists and dipeptidyl pepdidase-4 (DPP-4) inhibitors have been widely used for the treatment of type 2 diabetes (3). GLP1R agonists and DPP-4 inhibitors have also exhibited protective effects on β-cell apoptosis and other extrapancreatic tissues, such as the liver (4).

Clinical studies have demonstrated that liraglutide, a long-acting GLP1R agonist, significantly improves glycemic control in type 2 diabetes patients (5–12). The major advantages of liraglutide for the treatment of diabetic patients, compared with other therapies, such as insulin or sulfonylurea, are a reduction in body weight and fewer episodes of hypoglycemia (13). Liraglutide exerts an acute effect on pancreatic β-cell insulin release in response to glucose predominantly in the presence of elevated blood glucose levels, thereby preventing excessive insulin secretion in normoglycemic states. GLP1R activation has also been suggested to reduce glucagon secretion, reducing hypoglycemia (14, 15). Liraglutide has also exhibited protective effects on pancreatic β-cells in rodent models (16, 17). Moreover, GLP1R activation may reduce hepatic gluconeogenesis (4, 18). However, the mechanisms underlying the glucose concentration-dependent facilitation of insulin secretion by liraglutide remain unclear.

ISSN Print 0013-7227 ISSN Online 1945-7170
Printed in U.S.A.

doi: 10.1210/en.2012-1165 Received February 10, 2012. Accepted April 16, 2012.
First Published Online May 8, 2012

Abbreviations: ALT, Alanine aminotransferase; Atr, atropine; CS, chlorisondamine; DPP-4, dipeptidyl pepdidase-4; FFA, free fatty acid; GLP-1, glucagon-like peptide-1; GLP1R, GLP-1 receptor; GSIS, glucose-stimulated insulin secretion; GTT, glucose tolerance test; ITT, insulin tolerance test; NPH, neutral protamine Hagedorn; P, postnatal day; TChol, total cholesterol; TG, triglyceride; WT, wild type.

Glucokinase, a member of the hexokinase family, is the main glucose sensor in β-cells (19). Glucose-stimulated insulin secretion (GSIS) from pancreatic β-cells depends critically on glucokinase activity, and inactivating mutations cause either maturity onset diabetes of the young 2 or permanent neonatal diabetes (20). Whether glucokinase is involved in the potentiation of insulin secretion by GLP1R agonists is uncertain. The expression of glucokinase in β-cells is critical for the maintenance of glycemic control (21). We previously reported the characteristics of β-cell-specific glucokinase-deficient ($Gck^{-/-}$) mice, in which the neuron and β-cell-specific exon was disrupted (22). Mice that were heterozygous for β-cell glucokinase ($Gck^{+/-}$) exhibited impaired insulin secretion and manifested mild hyperglycemia, whereas mice that were homozygous for β-cell glucokinase ($Gck^{-/-}$) exhibited severe hyperglycemia and died within 1 wk after birth as a result of defective insulin secretion in response to glucose (22).

In this study, we used $Gck^{-/-}$ neonatal mice to evaluate the role of β-cell glucokinase in the actions of liraglutide and the effects on the survival rate, metabolic parameters, and histology of the endocrine pancreas and liver.

Materials and Methods

Animals and animal care

We backcrossed $Gck^{+/-}$ mice with C57Bl/6J mice more than 10 times. Both the adult wild-type (WT) and $Gck^{+/-}$ mice were fed standard chow (MF; Oriental Yeast, Tokyo, Japan). To generate the $Gck^{-/-}$ mice, we crossed $Gck^{+/-}$ mice with each other. The neonatal *WT*, $Gck^{+/-}$, and $Gck^{-/-}$ mice were weaned normally, with most of the pups being preweaning period at 15 d after birth.

All the experiments were conducted on male littermates. All the animal procedures were performed in accordance with the institutional animal care guidelines and the guidelines of the Animal Care Committee of the Yokohama-City University. The animal housing rooms were maintained at a constant room temperature (25 C) and on a 12-h light (0700 h)/12-h dark (1900 h) cycle.

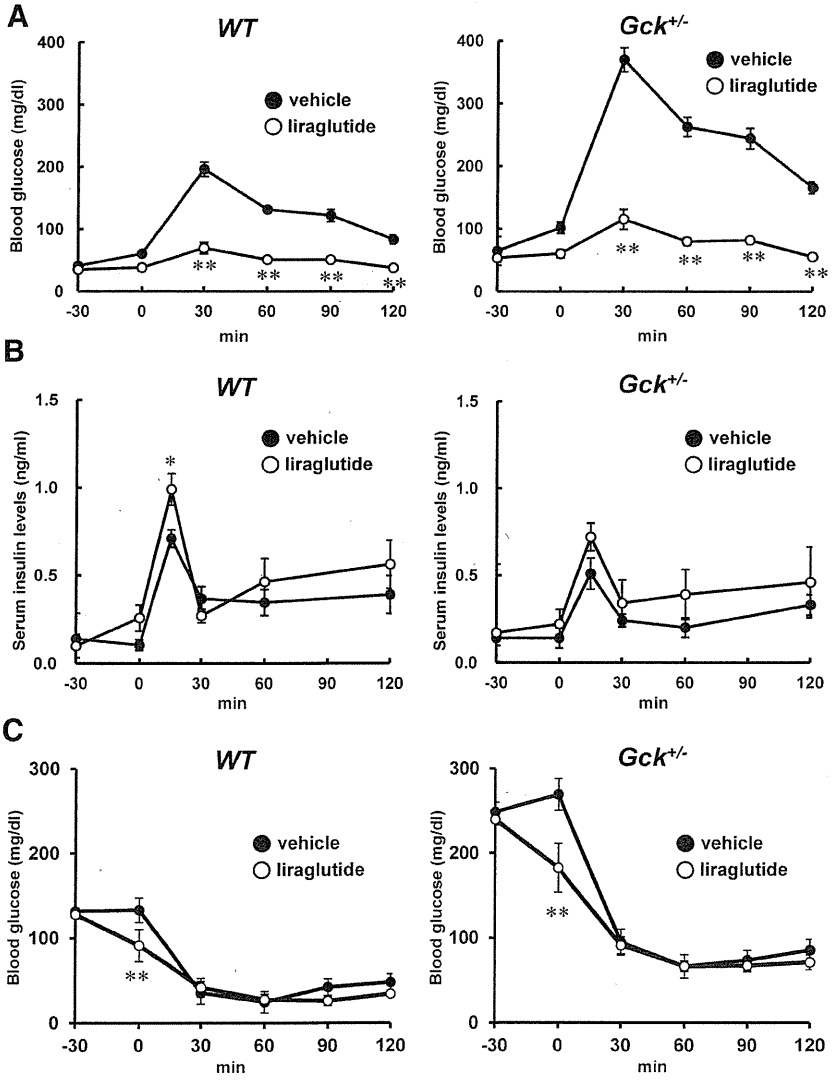

FIG. 1. A single administration of liraglutide significantly improved glucose tolerance in adult $Gck^{+/-}$ mice. GTT (A and B) (n = 6–10) and ITT (C) (n = 12–14) in 8-wk-old adult *WT* and $Gck^{+/-}$ mice. Liraglutide or the vehicle was administrated ip 30 min before the GTT or ITT. A and C, Plasma glucose levels. B, Serum insulin levels. *, $P < 0.05$; **, $P < 0.01$ *vs.* vehicle control.

Drugs

Liraglutide, a long-acting human insulin analog (insulin detemir), and intermediate-acting human insulin [neutral protamine Hagedorn (NPH)] in premanufactured sc injection pens were obtained from Novo Nordisk (Bagsvaerd, Denmark) and stored at 4 C until use. Saline solution was used as the vehicle control. For single administration experiments, the animals received either the vehicle or liraglutide (0.3 mg/kg ip) before oral glucose loading (1.5 mg/g) or insulin injection (0.75 mU/g). The ganglionic blocker chlorisondamine (CS) chloride (Sigma, St. Louis, MO) (3 mg/kg) and methyl atropine (Atr) (0.5 mg/kg; Sigma), a peripherally acting muscarinic blocker, were administered ip before the liraglutide injections. For the chronic administration of liraglutide in neonatal mice, *WT*, $Gck^{+/-}$, and $Gck^{-/-}$ pups received either the vehicle or liraglutide as twice daily sc injections (0900 and 2100 h) for 15 d after birth in the following manner: 0.1 mg/kg on

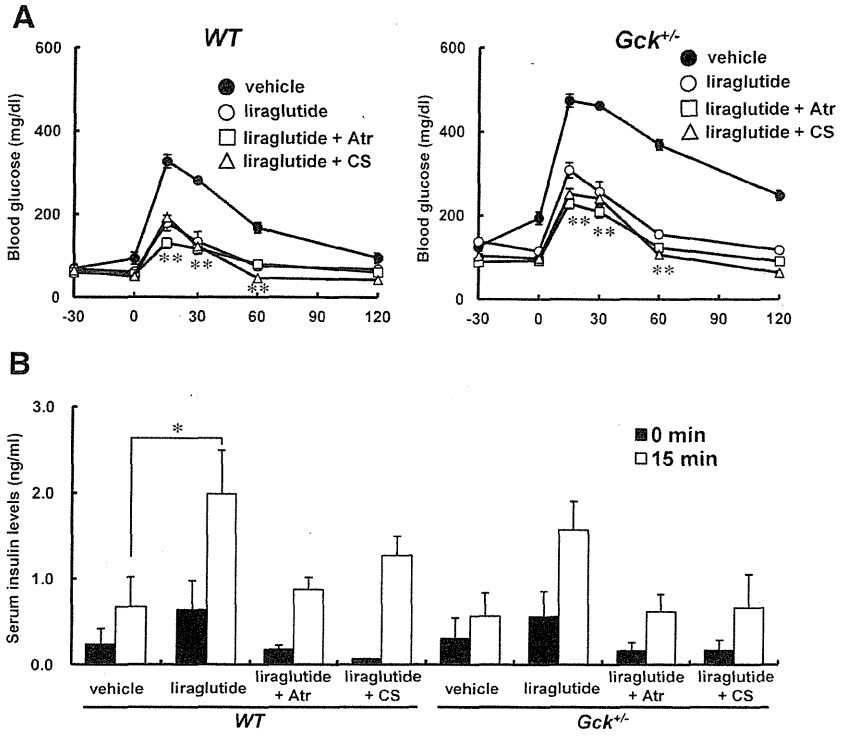

FIG. 2. Neither Atr nor CS affected the glucose lowering effects of liraglutide in either *WT* or $Gck^{+/-}$ mice. GTT in 8-wk-old adult *WT* and $Gck^{+/-}$ mice (n = 6–10). Liraglutide or the vehicle was administrated ip 30 min before the GTT. CS and Atr were administered ip just before the liraglutide injections. A, Plasma glucose levels. B, Serum insulin levels. *, $P < 0.05$ *vs.* vehicle control.

the first day (d 0), 0.2 mg/kg on the second day (d 1), and 0.3 mg/kg as the maintenance dose from the third day until the end of the experiment (d 2–15). For the double-dose administration of liraglutide in neonatal mice, the pups were treated with liraglutide using twice daily sc injections (0900 and 2100 h) for 15 d after birth in the following manner: 0.2 mg/kg on the first day [postnatal day (P)0], 0.4 mg/kg on the second day (P1), and 0.6 mg/kg as the maintenance dose from the third day until the end of the experiment (P2–P15). For insulin detemir or NPH injection, the pups were treated with insulin detemir or NPH using twice daily sc injections (0900 and 2100 h) for 15 d after birth in the following manner: 0.25 U/kg on the first day (d 0), 0.5 U/kg on the second day (d 1), and 0.75 U/kg as the maintenance dose from the third day until the end of the experiment (d 2–15).

Measurement of biochemical parameters and cytokines

The plasma glucose levels, blood insulin levels, triglyceride (TG) content in the liver, and glycogen content in the liver were determined using a Glutest Neo Super (Sanwa Chemical Co., Tokyo, Japan), insulin kit (Morinaga, Tokyo, Japan), Determiner-L TG II kit, and Determiner-GL-E kit (Wako Pure Chemical Industries, Osaka, Japan), respectively. The plasma alanine aminotransferase (ALT), free fatty acid (FFA), total cholesterol (TChol), low-density lipoprotein cholesterol, and TG levels were assayed using enzymatic methods (Wako Pure Chemical Industries).

Histological analysis

Liver sections were prepared and stained using hematoxylin (Wako Pure Chemical Industries) according to the manufacturer's instructions. More than 10 pancreatic tissue sections from each animal were analyzed after fixation and paraffin embedding. The sections were immunostained with antibodies to insulin (Santa Cruz Biotechnology, Inc., Santa Cruz, CA) and glucagon (Abcam, Cambridge, MA). Biotinylated secondary antibodies, a VECTASTAIN elite ABC kit, and a 3,3′-diaminobenzidine substrate kit (Vector Laboratories, Burlingame, CA) were used to examine sections using bright-field microscopy to determine the β-cell mass, and Alexa Fluor 488- and 555-conjugated secondary antibodies (Invitrogen, Carlsbad, CA) were used for fluorescence microscopy. All the images were acquired using a BZ-9000 microscope (Keyence, Osaka, Japan) or Carl Zeiss LSM 510 confocal laser-scanning microscope (Zeiss, Oberkochen, Germany). The proportion of the area of pancreatic tissue occupied by β-cells was calculated using BIOREVO software (Keyence), as described previously (23). Briefly, after staining a pancreatic section with insulin antibody, the insulin-positive area relative to the area of the entire pancreatic tissue was calculated for more than five sections per mouse.

Statistical analyses

All the data were reported as the mean ± SE and were analyzed using the Student's *t* test or ANOVA. Differences were considered significant if the *P* value was less than 0.05 (*).

Results

Single administration of liraglutide significantly improved glucose tolerance in both *WT* and $Gck^{+/-}$ mice

We previously demonstrated that $Gck^{+/-}$ islets exhibited the potentiation of GSIS via exendin-4, another GLP-1R agonist, at high glucose concentrations (23). To confirm the effects of liraglutide on $Gck^{+/-}$ mice, liraglutide (0.3 mg/kg) was injected ip 30 min before an oral glucose tolerance test (GTT) or an insulin tolerance test (ITT). Liraglutide significantly improved glucose tolerance in both *WT* and $Gck^{+/-}$ mice (Fig. 1A). The GSIS at 15 min after glucose loading was increased by liraglutide in *WT* mice but not in $Gck^{+/-}$ mice (Fig. 1B). Liraglutide did not affect insulin sensitivity after an insulin injection in both *WT* and $Gck^{+/-}$ mice (Fig. 1C). The insulinotropic actions of GLP-1 are reportedly affected by the blockade

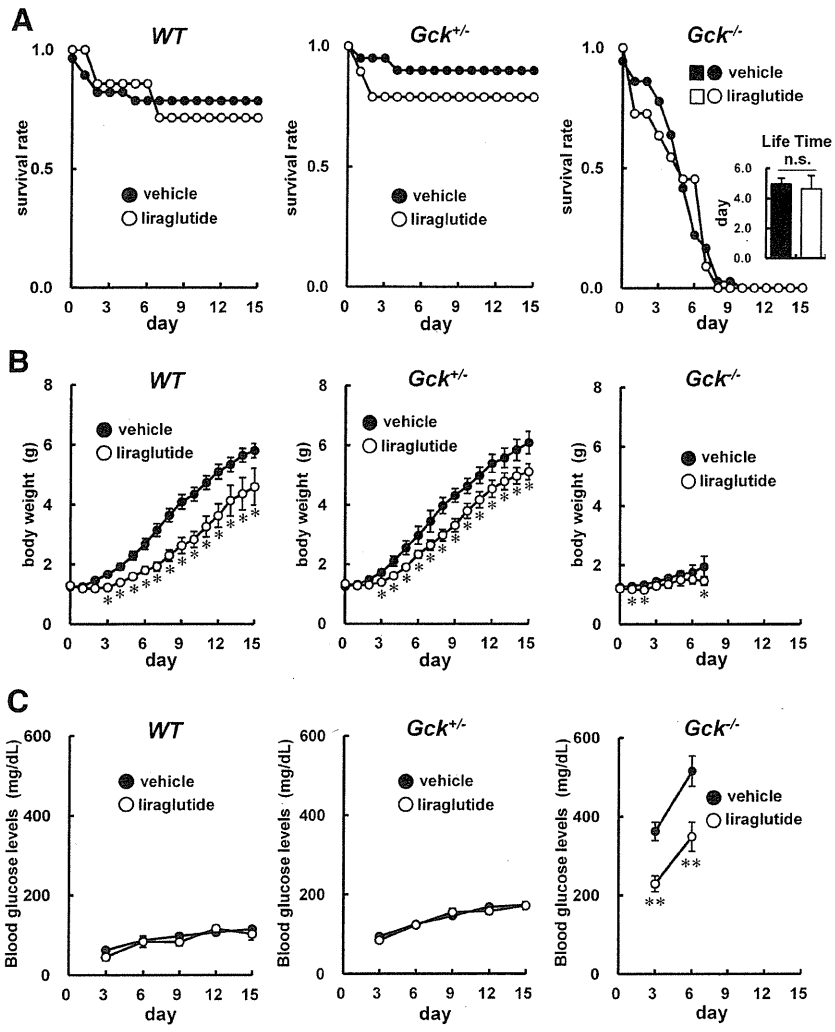

FIG. 3. Liraglutide did not prolong survival but reduced blood glucose levels in $Gck^{-/-}$ mice. Liraglutide or the vehicle was injected twice daily in *WT* (n = 22 and 9), $Gck^{+/-}$ (n = 40 and 19), and $Gck^{-/-}$ (n = 36 and 11) neonates, as described in *Materials and Methods*. A, Survival rate. B, Body weight changes. C, Plasma glucose levels. n.s., Not significant. *, $P < 0.05$; **, $P < 0.01$ *vs.* vehicle controls.

of the autonomic nervous system (24). The effects of autonomic nerve blockade on the action of liraglutide were evaluated by the ip administration of a ganglionic blocker, CS, or a peripheral muscarinic blocker, methyl Atr. Neither Atr nor CS affected the glucose-lowering effects of liraglutide in either *WT* or $Gck^{+/-}$ mice (Fig. 2A), although the insulin secretion at 15 min after glucose administration was reduced by both Atr and CS (Fig. 2B).

Liraglutide failed to prolong the survival of $Gck^{-/-}$ neonates

To evaluate the effects of liraglutide on the survival of severely hyperglycemic $Gck^{-/-}$ pups, *WT*, $Gck^{+/-}$, and $Gck^{-/-}$ pups were injected twice daily with either the vehicle or liraglutide, as described in *Materials and Methods*. Liraglutide did not affect the survival rate of any of the genotypes (Fig. 3A). The most notable finding was that almost all the $Gck^{-/-}$ mice died within 1 wk of birth despite the liraglutide treatment. Liraglutide also did not impinge on the mortality rate of *WT* and $Gck^{+/-}$ pups (mortality rate at P15 in vehicle group or liraglutide group, 0.21 or 0.29 in *WT* pups and 0.10 or 0.21 in $Gck^{+/-}$ pups). Liraglutide suppressed body weight gain in all the genotypes (Fig. 3B) and reduced the blood glucose levels in $Gck^{-/-}$ mice but not in the *WT* or $Gck^{+/-}$ mice (Fig. 3C). To exclude the possibility that the dose of liraglutide was insufficient to achieve an improvement, we injected the pups with a double dose of liraglutide. The double dose of liraglutide also did not improve the survival rate in $Gck^{-/-}$ mice (data not shown). We also assessed the effects of insulin detemir, a long-acting human insulin analog, on the survival rate of the pups. As expected, insulin detemir prolonged the survival rate and decreased the body weight gain in $Gck^{-/-}$ mice and reduced the blood glucose levels in all the genotypes (Supplemental Fig. 1, A–C, published on The Endocrine Society's Journals Online web site at http://endo.endojournals.org). These results indicated that liraglutide was unable to compensate for the early lethality caused by the profound insulin depletion in the $Gck^{-/-}$ mice.

Liraglutide did not affect GSIS in $Gck^{-/-}$ neonatal islets

We first measured the casual serum insulin levels at P2 or P3 in *WT*, $Gck^{+/-}$, and $Gck^{-/-}$ pups treated with twice daily injections of either vehicle or liraglutide, as described above. We previously reported that basal insulin secretion was preserved in $Gck^{-/-}$ pups (22). Consistent with this finding, the insulin levels were massively decreased, but not abolished, in these pups under casual nonfasting conditions (Fig. 4, A and B). Liraglutide failed to compensate for the striking reduction in the serum insulin levels at both P2 and P3 in $Gck^{-/-}$ mice (Fig. 4, A and B).

We next examined GSIS by islets isolated from *WT*, $Gck^{+/-}$, and $Gck^{-/-}$ pups at 3 d after birth (P3) in the presence or absence of liraglutide. As shown in Fig. 4C, the

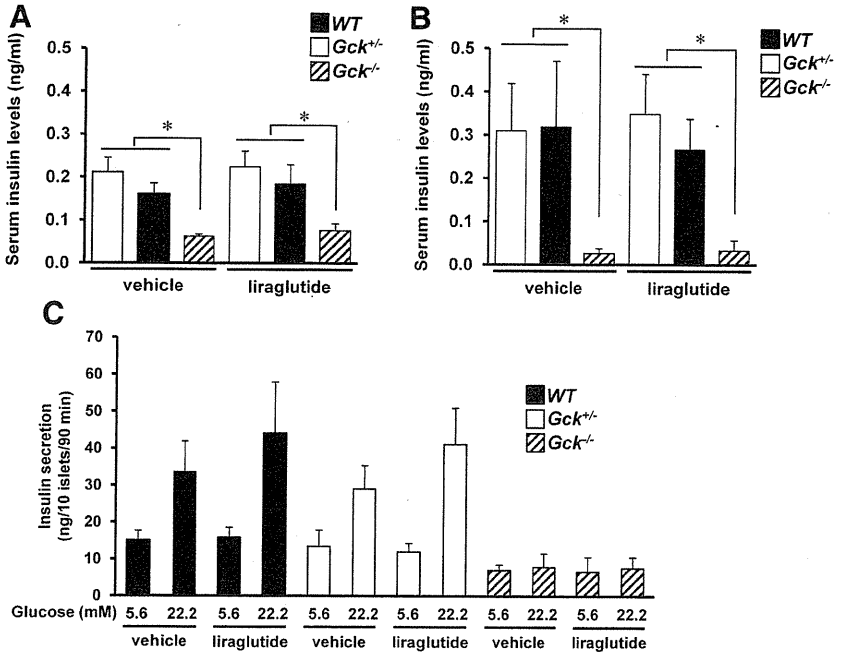

FIG. 4. Liraglutide did not exert its effects on insulin secretion in $Gck^{-/-}$ mice. Concentration of serum insulin (ng/ml) under nonfasting conditions in the groups of mice indicated at 2 d (A) or 3 d (B) after birth (n = 4–5). C, Insulin secretion by the islets of 3-d-old *WT* mice, $Gck^{+/-}$ mice, or $Gck^{-/-}$ mice in response to 5.6 or 22.2 mM glucose in the presence or absence of 1000 nM liraglutide. The results are shown as nanograms of insulin/10 islets/90 min (n = 5–7). *, $P < 0.05$.

P3 $Gck^{-/-}$ islets exhibited impaired insulin secretion at both low and high glucose concentrations, and their responses to glucose were diminished. Although insulin secretion at a glucose concentration of 22.2 mM showed a mild increment in the presence of liraglutide in islets from P3 *WT* and $Gck^{+/-}$ mice, liraglutide had no effect on insulin secretion from $Gck^{-/-}$ islets (Fig. 4C). About 50–70% of the insulin secretion in the presence of potassium chloride was detected in P3 $Gck^{-/-}$ islets, compared with P3 *WT* and $Gck^{+/-}$ islets (data not shown).

These results implied that glucokinase plays a critical role in liraglutide-induced insulin secretion from β-cells.

Elevations of plasma ALT, FFA, and TG were transiently prevented by liraglutide in $Gck^{-/-}$ mice

A previous report demonstrated that both TChol and TG levels were elevated in neonatal systemic glucokinase-deficient mice, and glucokinase expression in β-cells restored these levels (21). We determined the plasma ALT, FFA, TChol, and TG levels at P0–P5 in *WT*, $Gck^{+/-}$, and $Gck^{-/-}$ pups. $Gck^{-/-}$ mice exhibited significant elevations in ALT, FFA, and TG until P2 (Supplemental Fig. 2). We next evaluated the effects of intermediate-acting human insulin (NPH) or liraglutide on the lipid profiles of these mice. NPH prevented the elevation in ALT, and liraglutide averted the increases in the ALT, FFA, and TG levels at P2 (Fig. 5A), but not at P4 (Fig. 5B), in $Gck^{-/-}$ mice. Liraglutide also reduced the plasma levels of FFA, TChol, and TG in both *WT* and $Gck^{+/-}$ mice at P15 (Supplemental Fig. 3). In adult mice, glucokinase haploinsufficiency in the β-cells did not affect the plasma ALT level or the lipid profiles (Supplemental Fig. 4).

Liraglutide transiently protected against hepatic steatosis in $Gck^{-/-}$ mice

Systemic glucokinase-deficient mice exhibited a significant reduction in liver glycogen stores and microvesicular steatosis, with an increase in vacuolization and lipid accumulation (21). We examined the liver TG content and the liver glycogen content in *WT*, $Gck^{+/-}$, and $Gck^{-/-}$ pups. $Gck^{-/-}$ mice manifested a significant increase in liver TG and a decrease in liver glycogen at P2 (Fig. 6, A and E, and Supplemental Fig. 5). Gross observation and histological analysis revealed fatty changes in the liver and steatosis with vacuolization in $Gck^{-/-}$ mice at P2 (Fig. 6, B and C). In agreement with the transient amelioration of the increases in ALT, FFA, and TG induced by liraglutide in $Gck^{-/-}$ mice, liraglutide restored the increase in liver TG and the decrease in liver glycogen at P2 (Fig. 6A), but not at P4 (Fig. 6E), in $Gck^{-/-}$ mice. Liver steatosis was also improved by liraglutide at P2 in $Gck^{-/-}$ mice (Fig. 6, B and C). Thus, liraglutide improved circulating lipids and hepatic steatosis in a β-cell glucokinase-independent fashion. Because liver glucokinase plays a key role in glycogen synthesis, we assessed the expression of glucokinase in the liver. P2$Gck^{-/-}$ mice exhibited a reduced expression of glucokinase in the liver, and liraglutide restored the expression level (Fig. 6D). The amelioration of the histological changes and the glucokinase expression level in the liver by liraglutide also disappeared at P4 in $Gck^{-/-}$ mice (data not shown).

Liraglutide delayed β-cell loss in $Gck^{-/-}$ mice

We next investigated the histological analysis of endocrine pancreas in *WT*, $Gck^{+/-}$, and $Gck^{-/-}$ pups. Although all genotypes exhibited similar islet morphologies at P2 (Fig. 7, A and B), a decrease in the β-cell mass and the β-cell ratio in the islet cells were observed in P4 $Gck^{-/-}$ mice, compared with *WT* and $Gck^{+/-}$ mice (Fig. 7, C and D). Liraglutide and NPH increased the β-cell mass and the β-cell ratio in islet cells in P4 $Gck^{-/-}$ mice (Fig. 7, C and D).

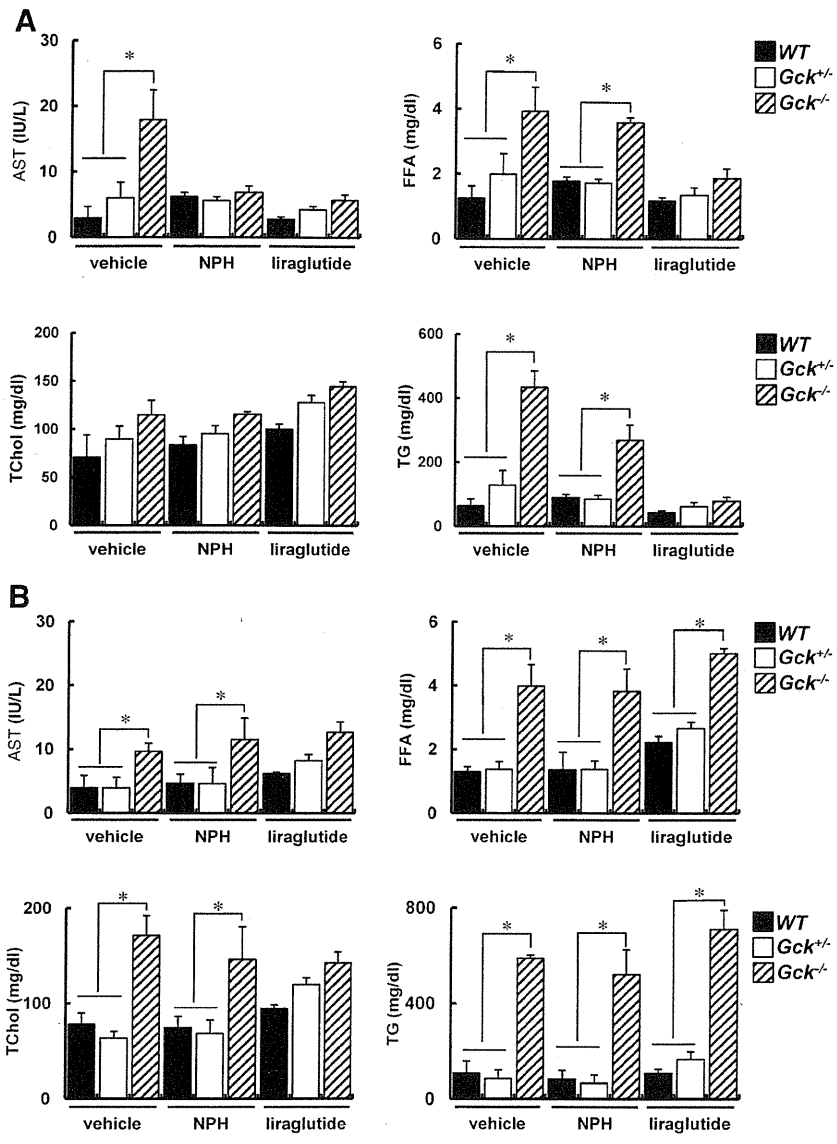

FIG. 5. Liraglutide improved biochemical parameters in $Gck^{-/-}$ mice at 2 d but not at 4 d after birth. Plasma ALT, FFA, TChol, and TG in *WT* mice, $Gck^{+/-}$ mice, and $Gck^{-/-}$ mice at 2 d (A) or 4 d (B) after birth (n = 7–8). *, $P < 0.05$.

Discussion

Glucokinase plays a central role as a glucose sensor in insulin-producing pancreatic islet β-cells and regulates GSIS (25, 26). β Cell-specific glucokinase-deficient ($Gck^{-/-}$) mice suffer from lethal hyperglycemia as a result of the lack of insulin secretion (22). In this study, we investigated the effects of liraglutide on β-cell-specific glucokinase-deficient $Gck^{-/-}$ neonatal mice.

Insulin detemir, but not liraglutide, prolonged the survival of $Gck^{-/-}$ neonatal mice. However, liraglutide decreased the blood glucose levels in $Gck^{-/-}$ pups and prevented body weight gain in all genotypes. Furthermore, a single administration of liraglutide reduced the blood glucose levels in an insulin concentration-independent manner in both *WT* and $Gck^{+/-}$ mice in the presence or absence of Atr and CS. These data suggest that the glucose-lowering effect of liraglutide is mediated, at least in part, by extrapancreatic effects (*e.g.* gastrointestinal motility), and liraglutide failed to compensate for the severe impairment of insulin secretion in $Gck^{-/-}$ neonatal mice. It is possible that the attainment of blood glucose levels by liraglutide is insufficient to affect survivability in $Gck^{-/-}$ pups, and more intense treatments may be required to enhance survivorship.

We demonstrated that liraglutide had no effects on insulin secretion in islets from $Gck^{-/-}$ neonatal mice. This result suggested that glucokinase is required for liraglutide action in insulin secretion from β-cells. In mice deficient in Kir6.2, an ATP-sensitive K^+ channel, pretreatment with GLP-1 potentiated insulin secretion and prevented an elevation in the blood glucose level after a GTT (27), whereas niflumic acid-sensitive ion channels are reportedly involved in the induction of GSIS by cAMP elevation after treatment with GLP-1 (28). Therefore, glucokinase may contribute to pathways other than Kir6.2-mediated depolarization in liraglutide-induced insulin secretion. The assessment of cAMP levels before and after treatment with liraglutide in $Gck^{-/-}$ islets is needed to clarify the mechanisms that are involved.

In human trials, liraglutide has been shown to induce significant reductions in T-Chol, low-density lipoprotein-cholesterol, and TG (6, 7, 9, 11). Liraglutide also lowered the TG levels in type 2 diabetes rats (17). We demonstrated the protective effects of liraglutide on elevations in ALT, FFA, and TG, and liraglutide improved hepatic steatosis in $Gck^{-/-}$ mice. However, the significance of aspartate aminotransferase (AAT or AST), ALT, or AAT/ALT ratio in fatty liver of neonatal mice remains unclear. Measurement of AAT may contribute to unravel the complexity of this mechanism of action in these neonates. In previous studies, GLP1R-mediated signals ameliorated fatty liver (29, 30), and DPP-4 inhibition protected against steatosis in a glucose-independent manner (4). Reductions in body weight and energy intake resulting from liraglutide administration have

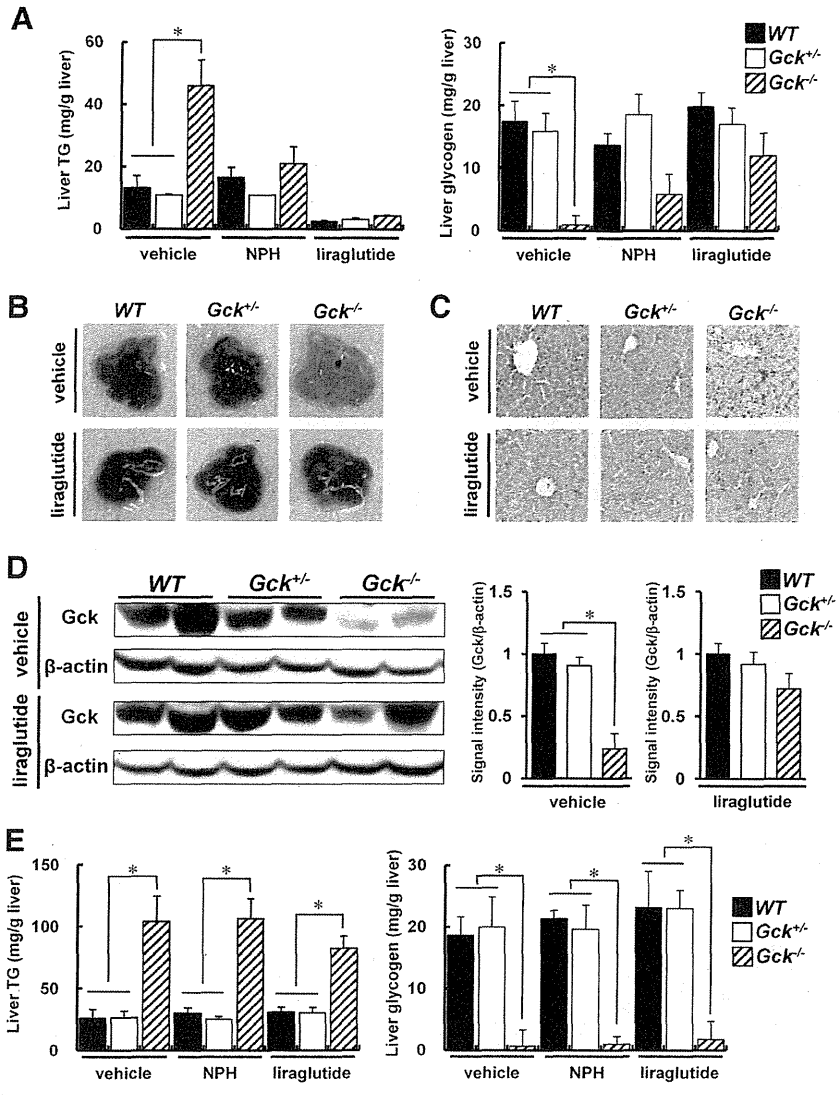

FIG. 6. Liraglutide protected against hepatic steatosis in $Gck^{-/-}$ mice at 2 d but not at 4 d after birth. Concentrations of liver TG (mg/g liver) and liver glycogen (mg/g liver) in the indicated groups of mice at 2 d (A) or 4 d (E) after birth (n = 5–8). B, Macroscopic observations of the liver from the indicated groups of mice at 2 d after birth. C, Hematoxylin staining of liver sections from the indicated groups of mice at 2 d after birth. D, *left panel*, Total cell extracts from the liver were subjected to immunoblotting for glucokinase (Gck) and β-actin as indicated at 2 d after birth. *Right panel*, Intensity of the Gck signals quantified by densitometry (ImageJ) and corrected by the intensity of the β-actin signal (n = 4). *, $P < 0.05$.

been previously reported (31, 32). The reduction in body weight gain observed in this study may have contributed to the improvements in the serum lipid parameters and the liver steatosis. One of the limitations of this study was its lack of weight-matched control groups to assess the influence of body weight changes on metabolic differences. In human hepatocytes, the expressions of GLP1R and GLP1R internalization by GLP-1 or exendin-4 have been reported (33). Additionally, GLP-1 reportedly suppresses hepatic lipogenesis via the activation of the AMP-activated protein kinase pathway in rats (34), raising the possibility that the prevention of liver steatosis by liraglutide was due to a glucokinase-independent direct action of GLP-1 on the liver. Liraglutide may be beneficial for the treatment of fatty liver even in patients in whom treatment with liraglutide does not lead to glycemic control.

Because glucokinase expression in the liver is dependent on insulin, hepatic glucokinase expression was diminished in $Gck^{-/-}$ mice, regardless of the intact regulation of gene expression in the liver. Our data, however, indicated that the restoration of glucokinase expression in the liver by liraglutide is not induced by the elevation of serum insulin levels. Furthermore, a single administration of liraglutide by ip injection did not affect glucokinase expression in the liver, although a single administration of insulin significantly increased glucokinase expression (data not shown). Sterol regulatory element binding protein-1c, peroxisome proliferator-activated receptor-γ, liver X receptor-α, small heterodimer partner, and PPARγ coactivator-1α are also involved in the regulation of glucokinase gene transcription in the liver (35, 36). However, glucokinase gene expression induced by hormones other than insulin has been less well characterized. The reduction of serum glucagon levels by liraglutide may have contributed to the suppression of cAMP elevation in hepatocytes, resulting in an increase in glucokinase expression. Because the amelioration of glucokinase expression in the liver by liraglutide was also transient, glucokinase expression might have been regulated by the serum FFA and TG levels through genes controlling lipid metabolism in the liver. Further study is required to unravel the complex interactions involved in the regulation of glucokinase expression in the liver.

Liraglutide also protected against β-cell loss without increasing insulin secretion in $Gck^{-/-}$ mice. Numerous reports have suggested that GLP1R activation has protective effects against β-cell damage (37). Our results suggest that liraglutide may also protect β-cells in the absence of glucokinase or irrespective of insulin secretion. The reduction in serum lipid levels may contribute to the avoidance of lipotoxicity in β-cells.

In summary, we demonstrated that β-cell glucokinase is required for liraglutide-induced increments in insulin secre-

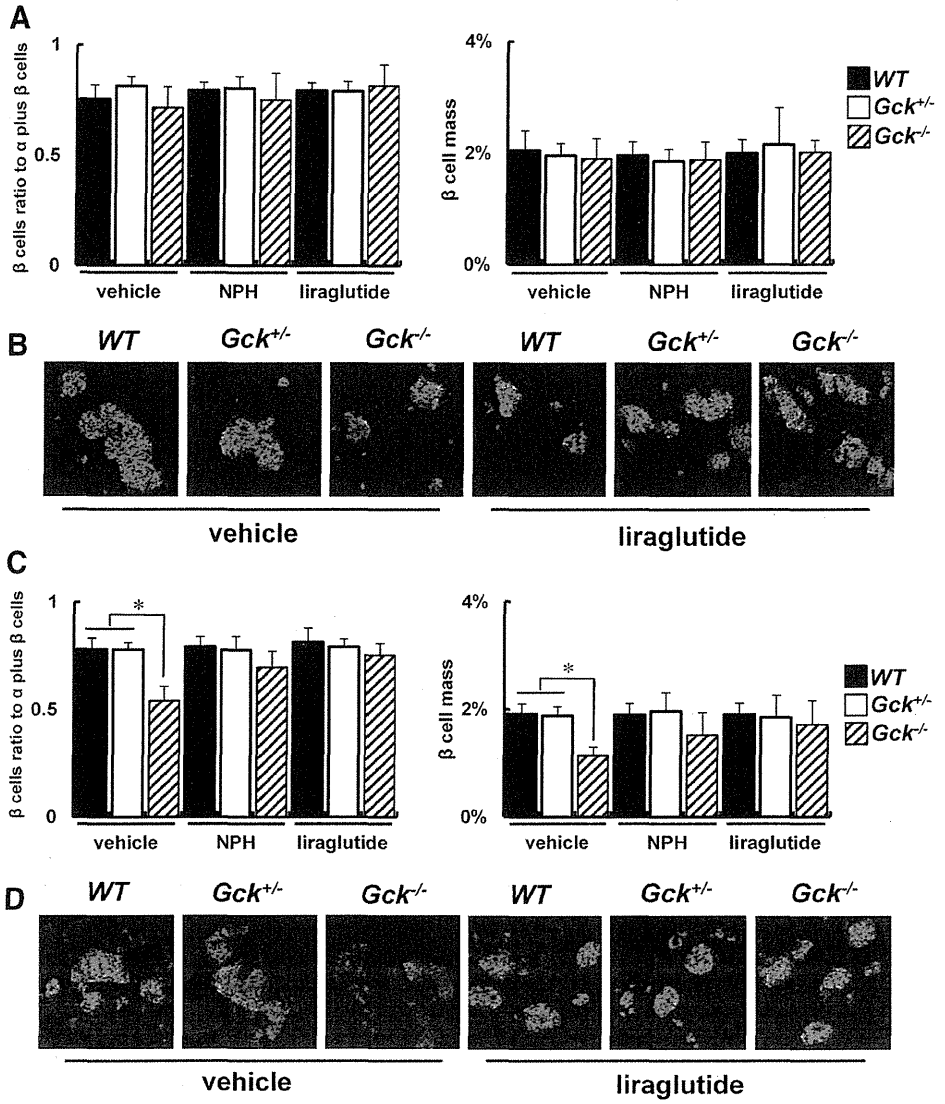

FIG. 7. Liraglutide protected against β-cell loss in $Gck^{-/-}$ mice until 4 d after birth. Quantification of β-cell mass as a proportion of the total α-cell plus β-cell mass in the islet (*left*) and the β-cell mass is shown as a proportion of the area of the entire pancreas (*right*) in the indicated groups of mice at 2 d (A) or 4 d (C) after birth ($n = 4–6$). Representative pancreatic sections stained with antibodies for insulin (*green*) and glucagon (*red*) are shown. The experiments were performed in *WT* mice, $Gck^{+/-}$ mice, and $Gck^{-/-}$ mice at 2 d (B) or 4 d (D) after birth. *, $P < 0.05$.

tion. However, the serum lipid parameters, liver steatosis, and β-cell loss were improved by liraglutide in a glucokinase- and insulin-independent manner. Because GLP-1 is involved in many biological activities in the brain, endothelial cells, peripheral nerves, and blood cells, GLP1R activation may have multiple pleiotropic effects. The results of the current study suggest a novel therapeutic potential of liraglutide for noninsulinotropic effects in diabetic patients, but further research is needed to clarify the mechanisms that are involved.

Acknowledgments

We thank Mitsuyo Kaji and Eri Sakamoto for their excellent technical assistance and animal care, Misa Katayama for secretarial assistance, and Novo Nordisk (Bagsværd, Denmark) for providing the liraglutide and for encouraging our research.

Address all correspondence and requests for reprints to: Yasuo Terauchi, M.D., Ph.D., Department of Endocrinology and Metabolism, Graduate School of Medicine, Yokohama-City University, 3-9 Fuku-ura, Kanazawa-ku, Yokohama 236-0004, Japan. E-mail: terauchi-tky@umin.ac.jp.

This work was supported by Grants-in-Aid for Scientific Research (B)19390251 and (B)21390282 from the Ministry of Education, Culture, Sports, Science, and Technology of Japan, a grant for the Strategic Japanese-Danish Cooperative Program on Molecular Diabetology from the Japan Science and Technology Agency, a Medical Award from the Japan Medical Association, a Grant-in-Aid from the Japan Diabetes Foundation, a Grant-in-Aid from the Suzuken Memorial Foundation, a Grant-in-Aid

from the Naito Foundation, a Grant-in-Aid from the Uehara Memorial Foundation (Y.Te.), and a Grant-in-Aid for JSPS Fellows (to J.S.).

Disclosure Summary: The authors have nothing to disclose.

References

1. **Ahrén B** 2011 GLP-1 for type 2 diabetes. Exp Cell Res 317:1239–1245
2. **Nauck MA** 2011 Incretin-based therapies for type 2 diabetes mellitus: properties, functions, and clinical implications. Am J Med 124: S3–18
3. **Drucker DJ, Nauck MA** 2006 The incretin system: glucagon-like peptide-1 receptor agonists and dipeptidyl peptidase-4 inhibitors in type 2 diabetes. Lancet 368:1696–1705
4. **Shirakawa J, Fujii H, Ohnuma K, Sato K, Ito Y, Kaji M, Sakamoto E, Koganei M, Sasaki H, Nagashima Y, Amo K, Aoki K, Morimoto C, Takeda E, Terauchi Y** 2011 Diet-induced adipose tissue inflammation and liver steatosis are prevented by DPP-4 inhibition in diabetic mice. Diabetes 60:1246–1257
5. **Garber AJ** 2011 Long-acting glucagon-like peptide 1 receptor agonists: a review of their efficacy and tolerability. Diabetes Care 34(Suppl 2):S279–S284
6. **Marre M, Shaw J, Brändle M, Bebakar WM, Kamaruddin NA, Strand J, Zdravkovic M, Le Thi TD, Colagiuri S** 2009 Liraglutide, a once-daily human GLP-1 analogue, added to a sulphonylurea over 26 weeks produces greater improvements in glycaemic and weight control compared with adding rosiglitazone or placebo in subjects with type 2 diabetes (LEAD-1 SU). Diabet Med 26:268–278
7. **Nauck M, Frid A, Hermansen K, Shah NS, Tankova T, Mitha IH, Zdravkovic M, Düring M, Matthews DR** 2009 Efficacy and safety comparison of liraglutide, glimepiride, and placebo, all in combination with metformin, in type 2 diabetes: the LEAD (liraglutide effect and action in diabetes)-2 study. Diabetes Care 32:84–90
8. **Garber A, Henry R, Ratner R, Garcia-Hernandez PA, Rodriguez-Pattzi H, Olvera-Alvarez I, Hale PM, Zdravkovic M, Bode B** 2009 Liraglutide versus glimepiride monotherapy for type 2 diabetes (LEAD-3 Mono): a randomised, 52-week, phase III, double-blind, parallel-treatment trial. Lancet 373:473–481
9. **Zinman B, Gerich J, Buse JB, Lewin A, Schwartz S, Raskin P, Hale PM, Zdravkovic M, Blonde L** 2009 Efficacy and safety of the human glucagon-like peptide-1 analog liraglutide in combination with metformin and thiazolidinedione in patients with type 2 diabetes (LEAD-4 Met+TZD). Diabetes Care 32:1224–1230
10. **Russell-Jones D, Vaag A, Schmitz O, Sethi BK, Lalic N, Antic S, Zdravkovic M, Ravn GM, Simó R** 2009 Liraglutide vs insulin glargine and placebo in combination with metformin and sulfonylurea therapy in type 2 diabetes mellitus (LEAD-5 met+SU): a randomised controlled trial. Diabetologia 52:2046–2055
11. **Buse JB, Rosenstock J, Sesti G, Schmidt WE, Montanya E, Brett JH, Zychma M, Blonde L** 2009 Liraglutide once a day versus exenatide twice a day for type 2 diabetes: a 26-week randomised, parallel-group, multinational, open-label trial (LEAD-6). Lancet 374:39–47
12. **Pratley RE, Nauck M, Bailey T, Montanya E, Cuddihy R, Filetti S, Thomsen AB, Søndergaard RE, Davies M** 2010 Liraglutide versus sitagliptin for patients with type 2 diabetes who did not have adequate glycaemic control with metformin: a 26-week, randomised, parallel-group, open-label trial. Lancet 375:1447–1456
13. **Davies MJ, Kela R, Khunti K** 2011 Liraglutide—overview of the preclinical and clinical data and its role in the treatment of type 2 diabetes. Diabetes Obes Metab 13:207–220
14. **Baggio LL, Drucker DJ** 2007 Biology of incretins: GLP-1 and GIP. Gastroenterology 132:2131–2157
15. **De Marinis YZ, Salehi A, Ward CE, Zhang Q, Abdulkader F, Bengtsson M, Braha O, Braun M, Ramracheya R, Amisten S, Habib AM, Moritoh Y, Zhang E, Reimann F, Rosengren AH, Shibasaki T, Gribble F, Renström E, Seino S, Eliasson L, Rorsman P** 2010 GLP-1 inhibits and adrenaline stimulates glucagon release by differential modulation of N- and L-type Ca2+ channel-dependent exocytosis. Cell Metab 11:543–553
16. **Shimoda M, Kanda Y, Hamamoto S, Tawaramoto K, Hashiramoto M, Matsuki M, Kaku K** 2011 The human glucagon-like peptide-1 analogue liraglutide preserves pancreatic β cells via regulation of cell kinetics and suppression of oxidative and endoplasmic reticulum stress in a mouse model of diabetes. Diabetologia 54:1098–1108
17. **Cummings BP, Stanhope KL, Graham JL, Baskin DG, Griffen SC, Nilsson C, Sams A, Knudsen LB, Raun K, Havel PJ** 2010 Chronic administration of the glucagon-like peptide-1 analog, liraglutide, delays the onset of diabetes and lowers triglycerides in UCD-T2DM rats. Diabetes 59:2653–2661
18. **Abu-Hamdah R, Rabiee A, Meneilly GS, Shannon RP, Andersen DK, Elahi D** 2009 Clinical review: the extrapancreatic effects of glucagon-like peptide-1 and related peptides. J Clin Endocrinol Metab 94:1843–1852
19. **Matschinsky F, Liang Y, Kesavan P, Wang L, Froguel P, Velho G, Cohen D, Permutt MA, Tanizawa Y, Jetton TL, et al** 1993 Glucokinase as pancreatic β cell glucose sensor and diabetes gene. J Clin Invest 92:2092–2098
20. **Osbak KK, Colclough K, Saint-Martin C, Beer NL, Bellanné-Chantelot C, Ellard S, Gloyn AL** 2009 Update on mutations in glucokinase (GCK), which cause maturity-onset diabetes of the young, permanent neonatal diabetes, and hyperinsulinemic hypoglycemia. Hum Mutat 30:1512–1526
21. **Grupe A, Hultgren B, Ryan A, Ma YH, Bauer M, Stewart TA** 1995 Transgenic knockouts reveal a critical requirement for pancreatic β cell glucokinase in maintaining glucose homeostasis. Cell 83:69–78
22. **Terauchi Y, Sakura H, Yasuda K, Iwamoto K, Takahashi N, Ito K, Kasai H, Suzuki H, Ueda O, Kamada N, et al** 1995 Pancreatic β-cell-specific targeted disruption of glucokinase gene. Diabetes mellitus due to defective insulin secretion to glucose. J Biol Chem 270: 30253–30256
23. **Shirakawa J, Amo K, Ohminami H, Orime K, Togashi Y, Ito Y, Tajima K, Koganei M, Sasaki H, Takeda E, Terauchi Y** 2011 Protective effects of dipeptidyl peptidase-4 (DPP-4) inhibitor against increased β cell apoptosis induced by dietary sucrose and linoleic acid in mice with diabetes. J Biol Chem 286:25467–25476
24. **Balkan B, Li X** 2000 Portal GLP-1 administration in rats augments the insulin response to glucose via neuronal mechanisms. Am J Physiol Regul Integr Comp Physiol 279:R1449–R1454
25. **Matschinsky FM** 2009 Assessing the potential of glucokinase activators in diabetes therapy. Nat Rev Drug Discov 8:399–416
26. **Matschinsky FM, Magnuson MA, Zelent D, Jetton TL, Doliba N, Han Y, Taub R, Grimsby J** 2006 The network of glucokinase-expressing cells in glucose homeostasis and the potential of glucokinase activators for diabetes therapy. Diabetes 55:1–12
27. **Miki T, Minami K, Shinozaki H, Matsumura K, Saraya A, Ikeda H, Yamada Y, Holst JJ, Seino S** 2005 Distinct effects of glucose-dependent insulinotropic polypeptide and glucagon-like peptide-1 on insulin secretion and gut motility. Diabetes 54:1056–1063
28. **Fujimoto W, Miki T, Ogura T, Zhang M, Seino Y, Satin LS, Nakaya H, Seino S** 2009 Niflumic acid-sensitive ion channels play an important role in the induction of glucose-stimulated insulin secretion by cyclic AMP in mice. Diabetologia 52:863–872
29. **Sharma S, Mells JE, Fu PP, Saxena NK, Anania FA** 2011 GLP-1 analogs reduce hepatocyte steatosis and improve survival by enhancing the unfolded protein response and promoting macroautophagy. PLoS One 6:e25269
30. **Gupta AC, Chaudhory AK, Sukriti, Pande C, Sakhuja P, Singh Y, Basir SF, Sarin SK** 2010 Peroxisome proliferators-activated receptor γ2 Pro12Ala variant is associated with body mass index in non-alcoholic fatty liver disease patients. Hepatol Int 5:575–580

31. **Larsen PJ, Fledelius C, Knudsen LB, Tang-Christensen M** 2001 Systemic administration of the long-acting GLP-1 derivative NN2211 induces lasting and reversible weight loss in both normal and obese rats. Diabetes 50:2530–2539
32. **Raun K, von Voss P, Gotfredsen CF, Golozoubova V, Rolin B, Knudsen LB** 2007 Liraglutide, a long-acting glucagon-like peptide-1 analog, reduces body weight and food intake in obese candy-fed rats, whereas a dipeptidyl peptidase-IV inhibitor, vildagliptin, does not. Diabetes 56:8–15
33. **Gupta NA, Mells J, Dunham RM, Grakoui A, Handy J, Saxena NK, Anania FA** 2010 Glucagon-like peptide-1 receptor is present on human hepatocytes and has a direct role in decreasing hepatic steatosis in vitro by modulating elements of the insulin signaling pathway. Hepatology 51:1584–1592
34. **Ben-Shlomo S, Zvibel I, Shnell M, Shlomai A, Chepurko E, Halpern Z, Barzilai N, Oren R, Fishman S** 2011 Glucagon-like peptide-1 reduces hepatic lipogenesis via activation of AMP-activated protein kinase. J Hepatol 54:1214–1223
35. **Kim TH, Kim H, Park JM, Im SS, Bae JS, Kim MY, Yoon HG, Cha JY, Kim KS, Ahn YH** 2009 Interrelationship between liver X receptor α, sterol regulatory element-binding protein-1c, peroxisome proliferator-activated receptor γ, and small heterodimer partner in the transcriptional regulation of glucokinase gene expression in liver. J Biol Chem 284:15071–15083
36. **Zhu LL, Liu Y, Cui AF, Shao D, Liang JC, Liu XJ, Chen Y, Gupta N, Fang FD, Chang YS** 2010 PGC-1α coactivates estrogen-related receptor-α to induce the expression of glucokinase. Am J Physiol Endocrinol Metab 298:E1210–E1218
37. **Asmar M, Holst JJ** 2010 Glucagon-like peptide 1 and glucose-dependent insulinotropic polypeptide: new advances. Curr Opin Endocrinol Diabetes Obes 17:57–62

Adiponectin Regulates Cutaneous Wound Healing by Promoting Keratinocyte Proliferation and Migration via the ERK Signaling Pathway

Sayaka Shibata,* Yayoi Tada,* Yoshihide Asano,* Carren S. Hau,* Toyoaki Kato,* Hidehisa Saeki,* Toshimasa Yamauchi,† Naoto Kubota,† Takashi Kadowaki,† and Shinichi Sato*

Diabetic patients are at high risk of developing delayed cutaneous wound healing. Adiponectin plays a pivotal role in the pathogenesis of diabetes and is considered to be involved in various pathological conditions associated with diabetes; however, its role in wound repair is unknown. In this study, we elucidated the involvement of adiponectin in cutaneous wound healing in vitro and in vivo. Normal human keratinocytes expressed adiponectin receptors, and adiponectin enhanced proliferation and migration of keratinocytes in vitro. This proliferative and migratory effect of adiponectin was mediated via AdipoR1/AdipoR2 and the ERK signaling pathway. Consistent with in vitro results, wound closure was significantly delayed in adiponectin-deficient mice compared with wild-type mice, and more importantly, keratinocyte proliferation and migration during wound repair were also impaired in adiponectin-deficient mice. Furthermore, both systemic and topical administration of adiponectin ameliorated impaired wound healing in adiponectin-deficient and diabetic *db/db* mice, respectively. Collectively, these results indicate that adiponectin is a potent mediator in the regulation of cutaneous wound healing. We propose that upregulation of systemic and/or local adiponectin levels is a potential and very promising therapeutic approach for dealing with diabetic wounds. *The Journal of Immunology*, **2012, 189: 3231–3241.**

Adipose tissue, located beneath the skin, was initially recognized merely as a site of energy storage. However, increasing evidence indicates that adipose tissue secretes various bioactive molecules and exerts multiple functions in concert with the epidermis and dermis via endo-, para-, and autocrine pathways (1, 2). Adipose tissue is now considered to be a key participant in the development of skin pathophysiology.

Bioactive molecules secreted from adipocytes are termed adipokines. Most adipokines, including TNF-α, IL-6, and resisitin, increase the risk of metabolic syndrome (3). In contrast, another adipokine, adiponectin, ameliorates insulin resistance and mediates antidiabetic effects in liver and skeletal muscle (4, 5). Adiponectin-deficient mice exhibit insulin resistance and glucose intolerance. Administration of adiponectin increases glucose uptake and fat oxidation in muscle, reduces glucose production in liver, and improves insulin sensitivity (6). Thus, adiponectin is a crucial factor in the pathogenesis of diabetes. Adiponectin is present at relatively high concentrations 3–30 μg/ml in circulation, and adiponectin levels are lower in obese and type 2 diabetes patients (7). Accumulated evidence shows that adiponectin is involved in the various pathological conditions associated with diabetes, such as arterial sclerosis, nephropathy, collateral vessel development, and ocular complications (8–10).

Diabetic patients frequently suffer from severely impaired wound healing, with a lifetime risk of 15% for developing diabetic skin ulcerations (11). Diabetic ulcers have a poor prognosis, and 15–27% of all diabetic ulcers lead to the surgical removal of bone (12). However, the mechanisms underlying impaired wound healing in diabetes are poorly understood (13). Wound healing involves a complex biological and molecular cascade of events, including inflammation, granulation tissue formation, re-epithelialization, and angiogenesis (14). Specifically, the re-epithelialization process is critical to optimal wound closure because of its role in wound contraction, which is mediated by keratinocyte proliferation and migration (14). These processes are regulated by the balance of various cytokines, chemokines, and growth factors released by adipose tissue as well as platelets, monocytes, and keratinocytes (1). Adipose tissue participates in cutaneous wound healing as a source of cytokines and growth factors, such as fibroblast growth factors (15), insulin-like growth factor (16), epidermal growth factor (EGF)-like growth factor (17), vascular endothelial growth factor, and angiopoietin-1 (18), and regulates skin wound repair in all layers of the skin via the endocrine/paracrine/autocrine pathways. Indeed, a recent study has shown that adipose tissue extracts, seeded over skin wounds, promotes wound repair (19). Furthermore, leptin, which is another representative adipokine and also secreted from adipocytes, induces keratinocyte proliferation and systemically and topically supplemented leptin improved re-epithelialization of wounds in leptin-deficient *ob/ob* mice and wild-type mice (20, 21).

In this study, to investigate the role of adiponectin during the cutaneous wound healing, we first focused on the functions of keratinocytes, key mediators of the re-epithelialization process, and

*Department of Dermatology, Faculty of Medicine, University of Tokyo, Tokyo 113-8655, Japan; and †Department of Metabolic Diseases, Faculty of Medicine, University of Tokyo, Tokyo 113-8655, Japan

Received for publication June 13, 2011. Accepted for publication July 19, 2012.

This work was supported by Health Science Research grants from the Ministry of Health, Labor and Welfare of Japan and grants from the Ministry of Education, Culture, Sports, Science and Technology-Japan.

Address correspondence and reprint requests to Dr. Yayoi Tada, Department of Dermatology, Faculty of Medicine, University of Tokyo, 7-3-1 Hongo, Bunkyo-ku, Tokyo 113-8655, Japan. E-mail address: ytada-tky@umin.ac.jp

The online version of this article contains supplemental material.

Abbreviations used in this article: AMPK, AMP-activated protein kinase; BHE, bovine hypothalamic extract; EGF, epidermal growth factor; HGF, hepatocyte growth factor; KO, knockout; qrt-PCR, quantitative real-time RT-PCR; siRNA, small interfering RNA.

www.jimmunol.org/cgi/doi/10.4049/jimmunol.1101739

performed functional analyses regarding proliferative and migratory effects. We further examined how adiponectin would be involved in vivo during the wound repair process, using a mouse model of excisional skin wound healing in adiponectin-deficient and diabetic *db/db* mice. The results of this study indicate that adiponectin enhances proliferation and migration of keratinocytes through AdipoR1/AdipoR2 and the ERK signaling pathway in vitro and that adiponectin regulates the skin wound healing process in vivo by promoting keratinocyte proliferation and migration.

Materials and Methods

Reagents

Recombinant human adiponectin was isolated and purified as described previously (22). We verified that purified recombinant adiponectin was free of endotoxin using an endotoxin detection kit (GenScript, Piscataway, NJ). Abs against ERK, p-ERK, p38, p-p38, JNK, p-JNK, Akt, p-Akt, and β-actin were obtained from Cell Signaling Technology (Beverly, MA). Abs against adiponectin, AdipoR1, and AdipoR2 were from Abcam (Cambridge, U.K.). Abs against Ki67 and loricrin were obtained from Novo Castra Laboratories (Newcastle, U.K.) and Covance (Berkeley, CA), respectively. PD98059, U0126, wortmannin, LY294002, SB203580, and SP600125 were also purchased from Cell Signaling Technology.

Cell culture

Normal human epidermal keratinocytes were cultured with MCDB153 medium supplemented with insulin (5 μg/ml), hydrocortisone (1 μM), ethanolamine (0.1 mM), phosphoethanolamine (0.1 mM), bovine hypothalamic extract (BHE) (50 μg/ml), and Ca^{2+} (0.1 mM) as described previously (23, 24). Third or fourth passage cells were used in this study.

RNA interference for adiponectin receptors

All transfections were done using Lipofectamine 2000 following the manufacturer's instructions (Invitrogen Life Technologies, Carlsbad, CA). Keratinocytes were plated in 6-well plates and cultured without antibiotics until reaching 30–50% subconfluency. AdipoR1/AdipoR2/calreticulin/T-cadherin and negative control small interfering RNA (siRNA) (Thermo Scientific Dharmacon, Lafayette, CO) were transfected into keratinocytes using Lipofectamine 2000. Medium was changed after 6 h after trans-

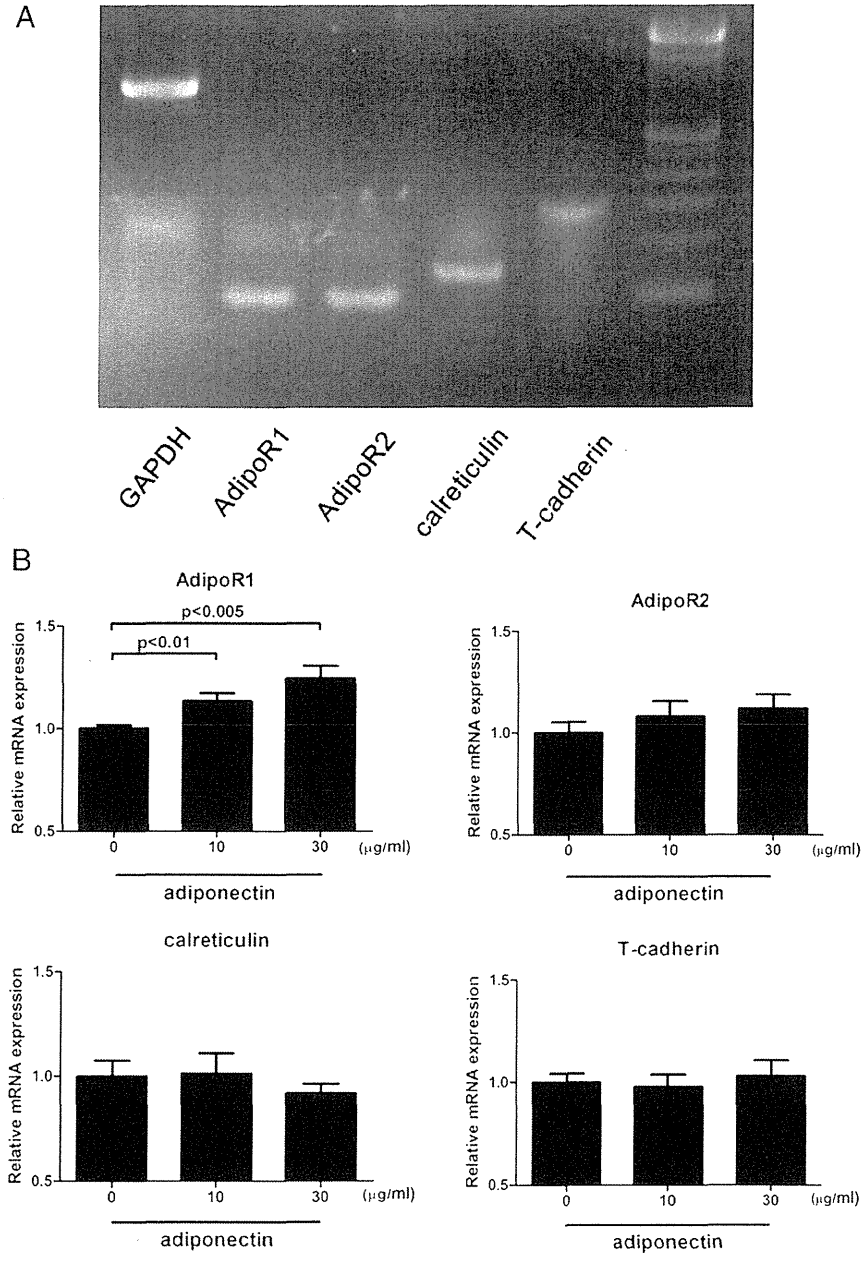

FIGURE 1. Expression of adiponectin receptors in normal human keratinocytes. (**A**) AdipoR1, AdipoR2, calreticulin, and T-cadherin mRNA expression in cultured primary normal human keratinocytes. Representative data from three independent experiments are shown. (**B**) Effect of adiponectin on AdipoR1/AdipoR2/calreticulin/T-cadherin mRNA expression in keratinocytes. Normal human keratinocytes were treated with indicated amounts of adiponectin for 9 h, and mRNA expression of AdipoR1/AdipoR2/calreticulin/T-cadherin was examined by qrt-PCR. Data are shown as mean ± SE (n = 8).

fection, and cells were incubated for another 24 h before subsequent analyses. Gene mRNA expression was examined by real-time RT-PCR analysis.

RT-PCR and quantitative real-time RT-PCR analysis

Total RNA was extracted from cultured keratinocytes and mouse back skin using an RNeasy Mini kit and RNeasy fibrous Tissue Mini kits, respectively (Qiagen, Germantown, MD), respectively. cDNA was synthesized using Superscript III First strand synthesis kits (Invitrogen).

For RT-PCR, synthesized cDNA was thermocycled for PCR amplification with 10 μM of each primer and 1.5 U Taq polymerase (Invitrogen). Primers for amplification, and the sizes of respective PCR products were as follows: AdipoR1, 5′-AATTCCTGAGCGCTTCTTTCCT-3′ and 5′-CATAGAAGTGGACAAAGGCTGC-3′; AdipoR2, 5′-TGCAGCCATTATAGTCTCCCAG-3′ and 5′-GAATGATTCCACTCAGGCCTAG-3′ (25); calreticulin, 5′-AAGTTCTACGGTGACGAGGAG-3′ and 5′-GTCGATGTTCTGCTCATGTTC-3′ (26); T-cadherin, 5′-GCCACGATCATGATCGATGAC-3′ and 5′-GTCTTCATTTTCCACTTTGA-3′ (27); and glyceraldehyde-3-phosphate dehydrogenase gene, 5′-TGAAGGTCGGAGTCAACGGATTTGGT-3′ and 5′-CATGTGGGCCATGAGGTCCACCAC-3′ (28). PCR was performed by 94°C for 5 min, 30 cycles of 94°C for 45 s, 60°C for 45 s, and 72°C for 45 s and a final extension at 72°C for 3 min. The PCR products were analyzed by electrophoresis on 2.5% agarose gels and stained with ethidium bromide, viewed by UV light.

For quantitative real-time RT-PCR (qrt-PCR), gene expression was quantified using TaqMan gene expression assay (Applied Biosystems, Warrington, U.K.). PCR conditions were 95°C for 10 min, 40 cycles of 94°C for 15 s, 60°C for 1 min. All samples were analyzed in parallel for glyceraldehyde-3-phosphate dehydrogenase gene expression as an internal control. The relative change in the levels of genes of interest was determined by the $2^{-\Delta\Delta CT}$ method.

Western blot analysis

Subconfluent keratinocytes were lysed in lysis buffer containing 20 mM Tris (pH 7.5), 150 mM NaCl, 1 mM EDTA, 1 mM EGTA, 1% Triton X-100, 2.5 mM sodium pyrophosphate, 1 mM glycerophosphate, 1 mM sodium orthovanadate, 1 mM PMSF, and 1 μg/ml leupeptin. Samples were dissolved in NuPAGE LDS Sample Buffer with NuPAGE Sample Reducing Agent (Invitrogen) and denatured by heating 5 min at 95°C. SDS-PAGE was performed with NuPAGE 4–12% Bis-Tris gels and MES running buffer (Invitrogen). After transfer to an Immobilon-P transfer membrane (Millipore, Bedford, MA), the membrane was incubated for 1 h at room temperature with blocking buffer, overnight at 4°C with the primary Ab, washed, and incubated for 1 h at room temperature with the appropriate secondary Ab. After washing, visualization was performed by ECL (Amersham Biosciences, Buckinghamshire, U.K.). In some experiments, phospho-ERK1/2 levels were quantified by densitometric analysis using ImageJ (available online) and normalized to the total ERK 1/2 levels.

MTT assay

Keratinocytes were seeded on 12-well plates at a density of 2×10^4 cells/well. The next day, the cells were fed MCDB153 medium lacking BHE, and the following day, they were fed once again with the same medium containing designated amounts of adiponectin. After 3 d, cell viability was assessed using an MTT assay kit (Roche Diagnostics, Basel, Switzerland), according to the manufacturer's instructions.

BrdU incorporation assay

Keratinocytes were seeded on 96-well plates at a density of 1×10^4 cells/well. After reaching subconfluency, the cells were fed MCDB153 medium lacking BHE. The following day, the cells were fed once again with the same medium containing designated amounts of adiponectin, EGF, and TGF-β and incubated for another 12 h. The cells were then incubated with medium containing BrdU for 2 h. BrdU incorporation was determined using a cell-proliferating ELISA kit (Roche Diagnostics, Basel, Switzerland), according to the manufacturer's instructions.

Boyden chamber assay

Keratinocyte migration was also assayed quantitatively with a Boyden chamber, as described previously (29). Designated amounts of adiponectin and hepatocyte growth factor (HGF) were added to the bottom wells of a 48-well Boyden chamber (Neuro Probe, Gaithersburg, MD), and a 10-μm pore-size polyvinylpyrrolidone-free polycarbonate membrane (Neuro Probe) was placed on the wells. The membrane was precoated with type I collagen (10 μg/ml in PBS; Nitta Gelatin) at room temperature for 1 h and then washed extensively with PBS. Subconfluent keratinocytes were harvested with trypsin–EDTA (0.05% trypsin and 0.5 mM EDTA) and resuspended in culture medium without BHE at 1×10^5 cells/ml. A 50-μl aliquot of the keratinocyte suspension (5000 cells/well) was added to the upper wells, and the chamber was incubated overnight at 37°C in a humidified atmosphere of air with 5% CO_2. The cells that adhered to the upper surface of the filter membrane were removed by scraping with a rubber blade, and the cells that moved through the filter and stayed on the lower surface of the membrane were considered to be migrated cells. The membrane was fixed with 10% buffered formalin overnight and then stained with crystal violet. The membrane was then mounted between two glass slides with 90% glycerol, and the number of migrated cells was counted under a microscope.

In vitro wound closure assay

Keratinocytes were seeded on 6-well plates at a density of 1×10^5 cells/well. After reaching subconfluency, wounds were created at the center of each well by scraping, and culture debris was removed by PBS washing. The remaining cells were cultured further with designated amounts of adiponectin and HGF. After 12 h, keratinocyte migration was observed under a phase contrast microscope. Wound closure was determined by identifying the front of cell migration and calculating a ratio of the migration area to the area of time 0.

Mice

Adiponectin-deficient mice were generated as described previously (6). BKS.Cg^{-} + Lepr db/+ Lepr db (*db/db*) were purchased from CLEA Japan (Tokyo, Japan). Mice were 7- to 10-wk-old for all experiments, and age-matched wild-type C57BL/6 mice (CLEA Japan) were used as controls for adiponectin-deficient and *db/db* mice. All mice were maintained under a 12-h light/12-h dark cycle in a specific pathogen-free barrier facility. All studies and procedures were approved by the Committee on Animal Experimentation of Tokyo University.

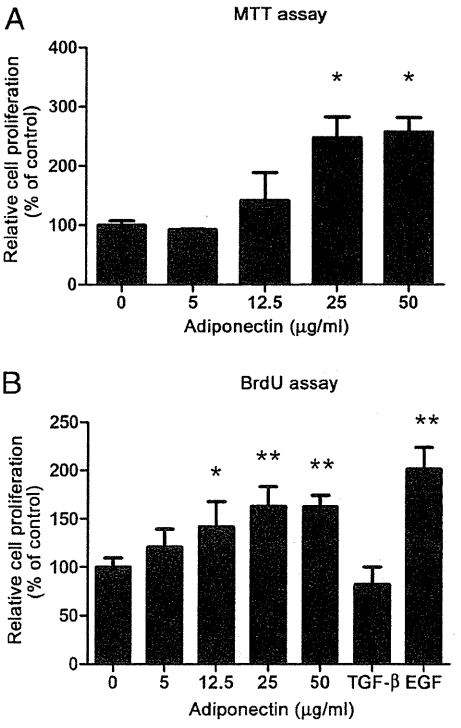

FIGURE 2. Proliferative effects of adiponectin in keratinocytes. (**A**) After incubation for 3 d with indicated amounts of adiponectin, cell viability was assessed using the MTT assay. Data are shown as mean ± SE ($n = 5$) and are representative of four independent experiments. *$p < 0.001$ versus unstimulated keratinocytes. (**B**) After incubation for 12 h with indicated amounts of adiponectin, EGF (positive control), and TGF-β (negative control), BrdU incorporation was determined by ELISA. Data are shown as mean ± SE ($n = 8$) and are representative of four independent experiments. *$p < 0.01$, **$p < 0.001$ versus unstimulated keratinocytes.

Wounding and macroscopic examination

Mice were anesthetized with diethyl ether, and their backs were shaved and wiped with 70% alcohol. Four full-thickness excisional wounds per mouse were made using a disposable sterile 6-mm biopsy punch (Maruho, Osaka, Japan), and mice were caged individually. No signs suggestive of local infection were detected in the wounded skin. We excluded wounds with extreme distortion, which did not permit a precise determination of their size. Areas of open wounds were traced onto a transparency and analyzed using ImageJ (available online).

Histological assessment of wound healing

Skin sections of wounds including a 2-mm rim of unwounded skin tissue were taken from murine back skin. The samples were formalin fixed and embedded in paraffin. Five-micrometer sections were stained with H&E. The epithelial gap, which represents distance between the leading edge of migrating keratinocytes, was measured under a light microscope. For the analyses of staining for adiponectin, AdipoR1/AdipoR2, Ki67, and loricrin, immunohistochemistry was performed using a Vectastain avidin/biotin complex kit (Vector Laboratories, Burlingame, CA), according to the manufacturer's instructions. The 5-μm sections were deparaffinized and rehydrated, endogeneous perioxidase activity was eliminated by blocking with hydrogen peroxide, and the tissue sections were immersed in citrated buffer and boiled for 10 min for Ag retrieval. The sections were then incubated with indicated Abs overnight at 4°C, followed by the incubation with biotinylated secondary Ab. The concentration of each primary Ab was first tested to determine the optimal sensitivity range. The immunoreactivity was visualized with diaminobenzidine, and the sections were counterstained with Mayer's hematoxylin.

Statistical analyses

Data obtained are presented as mean ± SE. Student *t* test was used for the statistical analysis of differences between two groups. One-way ANOVA with Dunnett's multiple comparison test was used for statistical analysis of the differences among multiple groups. A p value < 0.05 was considered to represent a significant difference.

Results

Adiponectin receptors are expressed in human keratinocytes and AdipoR1 expression is upregulated by adiponectin stimulation

AdipoR1 is expressed widely in various tissues, with the highest expression level in skeletal muscle, whereas AdipoR2 is most abundantly expressed in the liver (30). Recently, new receptors for adiponectin, calreticulin, and T-cadherin also have been identified and reported to be involved in adiponectin cellular signaling (31–34). We first investigated the expressions of these adiponectin receptors in normal human keratinocytes. Human keratinocytes expressed both AdipoR1/AdipoR2 as well as calreticulin and T-cadherin at the mRNA level (Fig. 1A). Adiponectin upregulated gene expression levels of AdipoR1 in a dose-dependent manner but not those of AdipoR2, calreticulin, or T-cadherin in keratinocytes (Fig. 1B).

Adiponectin enhances keratinocyte proliferation

We next investigated the effect of adiponectin on keratinocyte proliferation using the MTT and BrdU assays. The MTT assay quantifies viable cells, whereas the BrdU assay determines BrdU incorporation into newly synthesized DNA of actively proliferating cells. Adiponectin increased the number of viable keratinocytes (Fig. 2A) and BrdU uptake (Fig. 2B) in a dose-dependent manner, reaching a plateau at a concentration of 25 μg/ml. Because plasma adiponectin concentrations in healthy humans are ~3–30 μg/ml (36), the stimulatory effects of adiponectin were significant within physiological concentrations. EGF, a positive control, significantly induced keratinocyte proliferation in the BrdU assay, whereas TGF-β, a negative control, had no effect (37).

Adiponectin induces keratinocyte migration

After establishing that adiponectin stimulates keratinocyte proliferation, we next investigated the effect of adiponectin on keratinocyte migration using two types of in vitro assay systems. In the Boyden chamber assay, we quantitatively investigated adiponectin-induced migration. Various amounts of adiponectin and cultured human keratinocytes were added to the lower and upper chambers, respectively. After incubation overnight, the number of migrated cells was counted. Adiponectin significantly stimulated keratinocyte migration at concentrations of 12.5–50 μg/ml (Fig. 3A). HGF was used as a positive control, which induced an ~7-fold increase relative to control (38).

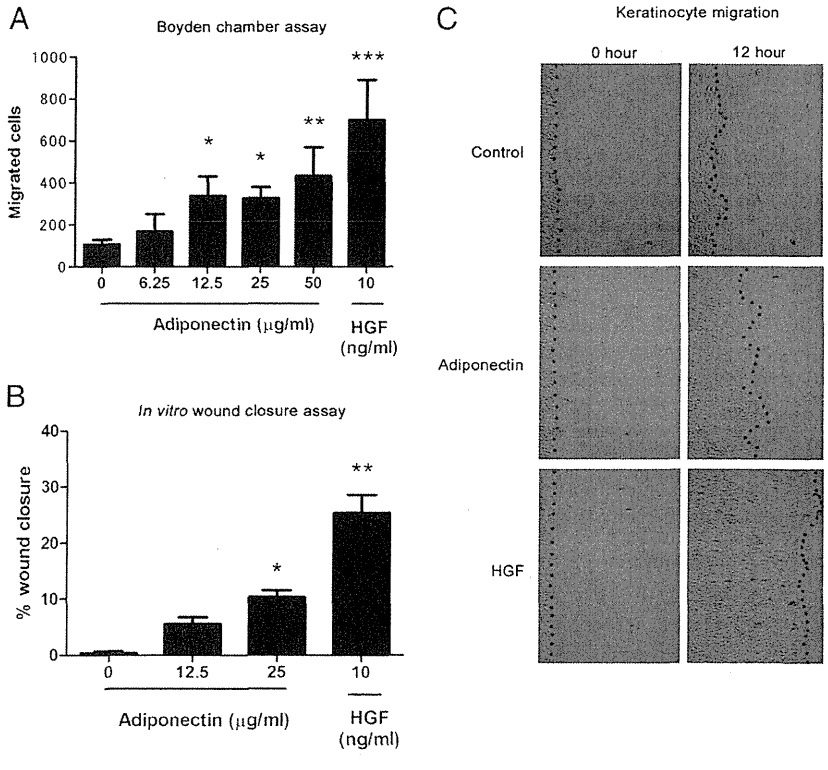

FIGURE 3. Migratory effects of adiponectin in keratinocytes. (**A**) Keratinocyte migration was assayed quantitatively using the Boyden chamber assay. Indicated amounts of adiponectin and HGF were added to the lower wells. After keratinocytes were added to the upper wells and incubated overnight, the migrated cells were counted. Data are shown as mean ± SE (n = 6) and are representative of four independent experiments. $*p < 0.05$, $**p < 0.01$, $***p < 0.001$ versus unstimulated keratinocytes. (**B**) Keratinocyte migration was assayed using the in vitro wound closure assay. After subconfluent keratinocytes were scraped and incubated with indicated amounts of adiponectin and HGF for 12 h, migration over the wound was measured. Data are shown as mean ± SE (n = 6) and are representative of three independent experiments. $*p < 0.01$, $**p < 0.001$ versus unstimulated keratinocytes. (**C**) Representative micrograph of keratinocytes directly after (*left panels*) or 12 h after (*right panels*) scraping (original magnification ×20).

Next, wounds were created in cultured keratinocytes by scraping (in vitro wounds). Keratinocytes were cultured with various concentrations of adiponectin or HGF. Acceleration of wound closure was observed in response to 25 μg/ml adiponectin 12 h after wounding (Fig. 3B, 3C).

The ERK signaling pathway is activated by adiponectin via AdipoR1/AdipoR2 in keratinocytes

MAPK is a well-known factor involved in cell proliferation (39–41). Akt and AMP-activated protein kinase (AMPK) are also known to enhance cell proliferation and suppress apotosis (10). Therefore, we investigated whether adiponectin could induce phosphorylation of MAPKs, Akt and AMPK in normal human keratinocytes. As shown in Fig. 4A, adiponectin (25 μg/ml) induced phosphorylation of ERK in keratinocytes. The peak activation occurred at 5 min after stimulation, and thereafter, the phosphorylation level gradually decreased. Adiponectin had no effect on the phosphorylation of the p38 MAPK, JNK, Akt, and AMPK (Fig. 4B). To confirm the specificity of the identified pathway, keratinocytes were pretreated with 75 μM MEK1 in-

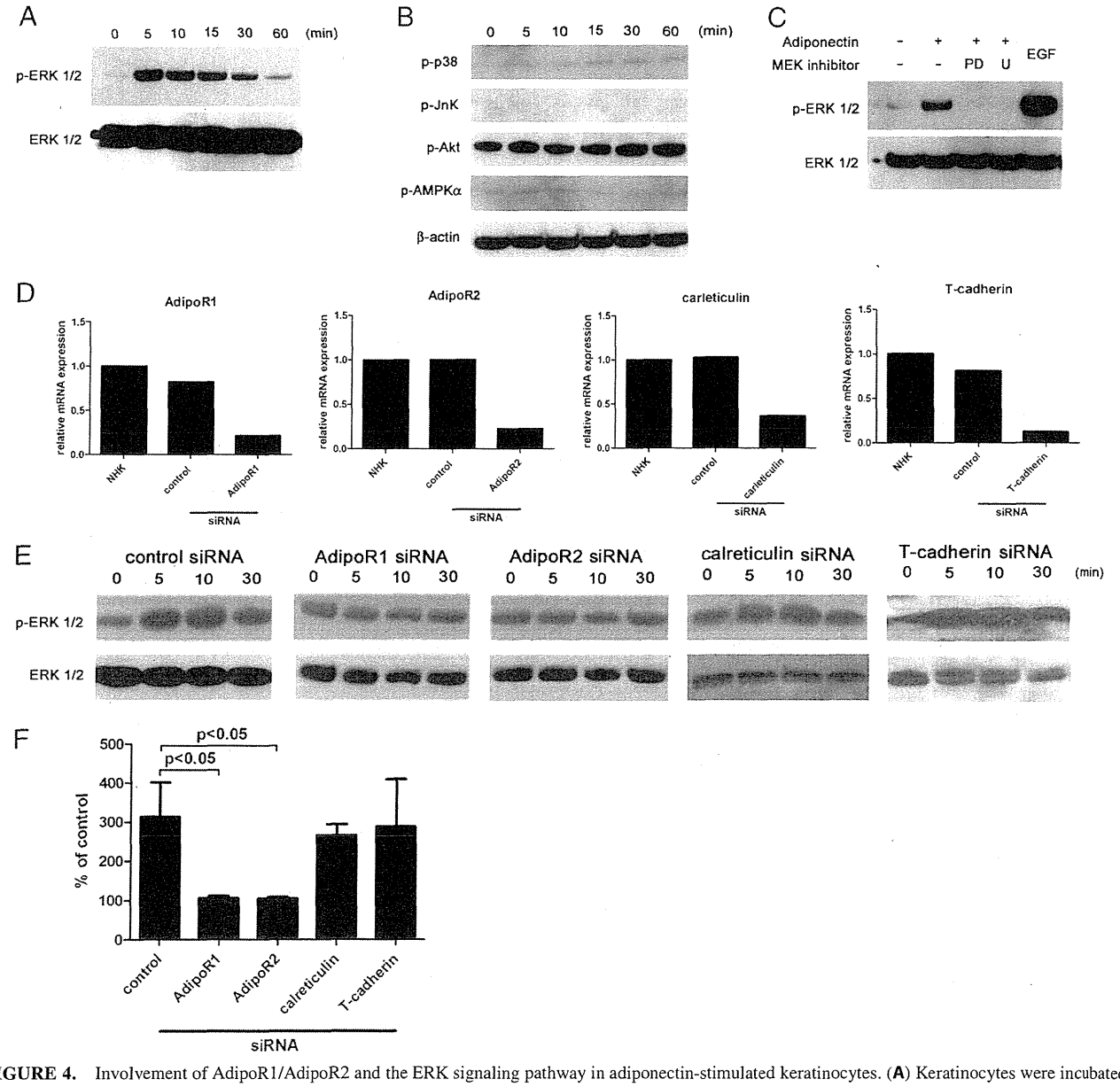

FIGURE 4. Involvement of AdipoR1/AdipoR2 and the ERK signaling pathway in adiponectin-stimulated keratinocytes. (**A**) Keratinocytes were incubated with adiponectin (25 μg/ml) for 0–60 min. The cell lysates were analyzed for phosphorylation of ERK1/2 by Western blotting. Results are representative of four independent experiments. (**B**) Keratinocytes were incubated with adiponectin (25 μg/ml) for 0–60 min. The cell lysates were analyzed for phosphorylation of p38 MAPK, JnK, Akt, and AMPK by Western blotting. Results are representative of four independent experiments. (**C**) Keratinocytes were pretreated with PD98059 (PD; 75 μM, MEK1 inhibitor) or U0126 (U; 10 μM, MEK1/2 inhibitor) for 30 min. After incubation with adiponectin (25 μg/ml) for 5 min, the cell lysates were analyzed for ERK1/2 phosphorylation by Western blotting. Results are representative of four independent experiments. (**D**) Keratinocytes were transfected with control siRNA or siRNA targeting AdipoR1/AdipoR2/calreticulin/T-cadherin. mRNA expression of these receptors in transfected cells was examined by qrt-PCR. Results are representative of three independent experiments. (**E**) Transfected cells were incubated with adiponectin (25 μg/ml) for 0–30 min. The cell lysates were analyzed for phosphorylation of ERK1/2 by Western blotting. Results are representative of three independent experiments. (**F**) Densitometry analysis of P5/P0 (P5, phospho-ERK protein expression levels/total ERK protein expression levels at 5 min after adiponectin stimulation; P0, phospho-ERK protein expression levels/total ERK protein expression levels before adiponectin stimulation), and data are expressed as mean ± SE (n = 3).

hibitor (PD98059) and 10 μM MEK1/2 inhibitor (U0126) for 30 min and then stimulated with adiponectin for 5 min. Both of these inhibitors blocked adiponectin-induced ERK phosphorylation (Fig. 4C). To determine whether the activation of the ERK signaling pathway by adiponectin is mediated through AdipoR1/AdipoR2/calreticulin/T-cadherin, keratinocytes were transfected with siRNAs of these receptors, and specific inhibition was performed. Control experiments have revealed that AdipoR1/AdipoR2/calreticulin/T-cadherin mRNA levels are reduced by >80% as evaluated by real-time RT-PCR analysis (Fig. 4D). Under these experimental conditions, inhibition of AdipoR1 or AdipoR2 completely suppressed adiponectin-induced ERK phosphorylation in keratinocytes (Fig. 4E, 4F). However, downregulation of calreticulin or T-cadherin did not significantly suppress adiponectin-induced ERK phosphorylation. These results indicate that 1) adiponectin activates the ERK signaling pathway through AdipoR1 and AdipoR2 and that 2) calreticulin or T-cadherin appear not to be involved in the ERK signaling pathway mediated by adiponectin in keratinocytes.

ERK signaling pathway mediates adiponectin-induced keratinocyte proliferation and migration

To investigate the role of the ERK signaling pathway in keratinocyte proliferation induced by adiponectin, we incubated keratinocytes with PD98059 (75 μM) or U0126 (10 μM) for 30 min before stimulation with adiponectin (25 μg/ml), and then, BrdU uptake was analyzed. Both of these inhibitors attenuated BrdU uptake induced by adiponectin, indicating that adiponectin-induced keratinocyte proliferation is mediated by the ERK pathway (Fig. 5A). Other kinase inhibitors (wortmannin and LY294002 for inhibition of PI3K, SB203580 for inhibition of p38 MAPK, and SP600125 for inhibition of JNK) did not affect adiponectin-induced proliferation. We further investigated whether the ERK signaling pathway would be involved in the keratinocyte migration induced by adiponectin. After the addition of PD98059 (75 μM) or U0126 (10 μM) to the lower chamber with adiponectin, keratinocyte migration was analyzed using the Boyden chamber assay. Both of the inhibitors blocked adiponectin-induced keratinocyte migration (Fig. 5B). These results suggest that the ERK signaling pathway mediated adiponectin-induced keratinocyte migration as well as proliferation.

Wound closure and keratinocyte re-epithelialization are significantly delayed in adiponectin-deficient mice

To further strengthen our in vitro results and to determine the role of adiponectin during cutaneous wound healing in vivo, we first examined the excisional wound skin repair process in adiponectin-deficient and wild-type mice. Full-thickness round wounds of 6 mm in diameter were made, and the kinetics of wound closure were evaluated as percentage of original wound areas. Adiponectin-deficient mice exhibited significantly impaired wound repair compared with wild-type mice from day 3 (Fig. 6A, 6B). All the wounds of wild-type mice healed within 9 d after wounding, whereas the wounds of adiponectin-deficient mice took more than 13 d to heal. Next, we focused on the re-epithelialization phase of wound healing, which involves keratinocyte proliferation and migration for wound contraction. To confirm the pattern of keratinocyte differentiation to be normal in the adiponectin-deficient mice skin, we first examined the expression of loricrin, a marker of late-phase keratinocyte differentiation, by immunohistochemistry. Loricrin expression in the keratinocytes was comparable between wild-type and adiponectin-deficient mice (Fig. 6C). Next, we performed immunohistochemistry for the proliferation marker

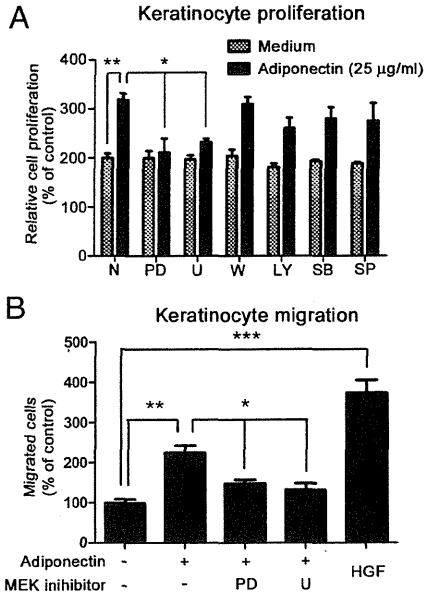

FIGURE 5. Involvement of the ERK signaling pathway in adiponectin-induced proliferation and migration of keratinocytes. (**A**) Keratinocytes were preincubated with PD98059 (PD; 75 μM), U0126 (U; 10 μM), wortmannin (W; 0.5 μM, PI3K inhibitor), LY294002 (LY; 10 μM, PI3K inhibitor), SB203580 (SB; 10 μM, p38 MAPK inhibitor), and SP600125 (SP; 10 μM, JNK inhibitor) or without inhibitors (N). After incubation with adiponectin for 12 h, keratinocyte proliferation was analyzed using the BrdU assay. Data are shown as mean ± SE (n = 8) and are representative of four independent experiments. *$p < 0.05$ versus medium treated with adiponectin (25 μg/ml), **$p < 0.001$ versus medium alone. (**B**) Indicated amounts of adiponectin with or without PD98059 (PD; 75 μM) and U0126 (U; 10 μM) were added to the lower wells. Keratinocyte migration was analyzed using the Boyden chamber assay. Data are shown as mean ± SE (n = 6) and are representative of three independent experiments. *$p < 0.05$ versus medium treated with adiponectin (25 μg/ml), **$p < 0.01$ and ***$p < 0.001$ versus medium alone.

Ki67 on the skin samples of the wound margins (20, 42). Distribution of Ki67-positive proliferating keratinocytes was more intensive in the wound margins of control wild-type mice compared with adiponectin knockout (KO) mice (Fig. 6D, 6E). Furthermore, the epithelial gap, the distance between the migrating edges of keratinocytes, was significantly wider in adiponectin-deficient mice compared with wild-type mice (Fig. 6A, 6F), suggesting that keratinocyte migration was significantly inhibited in adiponectin-deficient mice. These results are in accordance with the in vitro results regarding the proliferative and migratory functions of adiponectin in keratinocytes.

The gene expression of adiponectin and AdipoR1/AdipoR2 gradually increases during the wound healing process

To determine whether the local adiponectin and AdipoR1/AdipoR2 expression levels change during the wound healing process, we determined the changes in expression of these genes over time. Skin samples, taken immediately before (at day 0) and 3 and 6 d (days 3 and 6) after wounding, were analyzed by the qrt-PCR. We demonstrate in this study that adiponectin expression at the wound site gradually increased during the course of wound repair in wild-type mice (Fig. 7A), suggesting that adiponectin production might be upregulated sensing tissue damage of wounding. Immunohistochemistry of adiponectin showed that the sources of adiponectin are adipocytes and fibroblasts but not keratinocytes (Fig. 7B). Regarding adiponectin receptors, AdipoR1 and AdipoR2 mRNA expression also increased gradually after wounding in both wild-

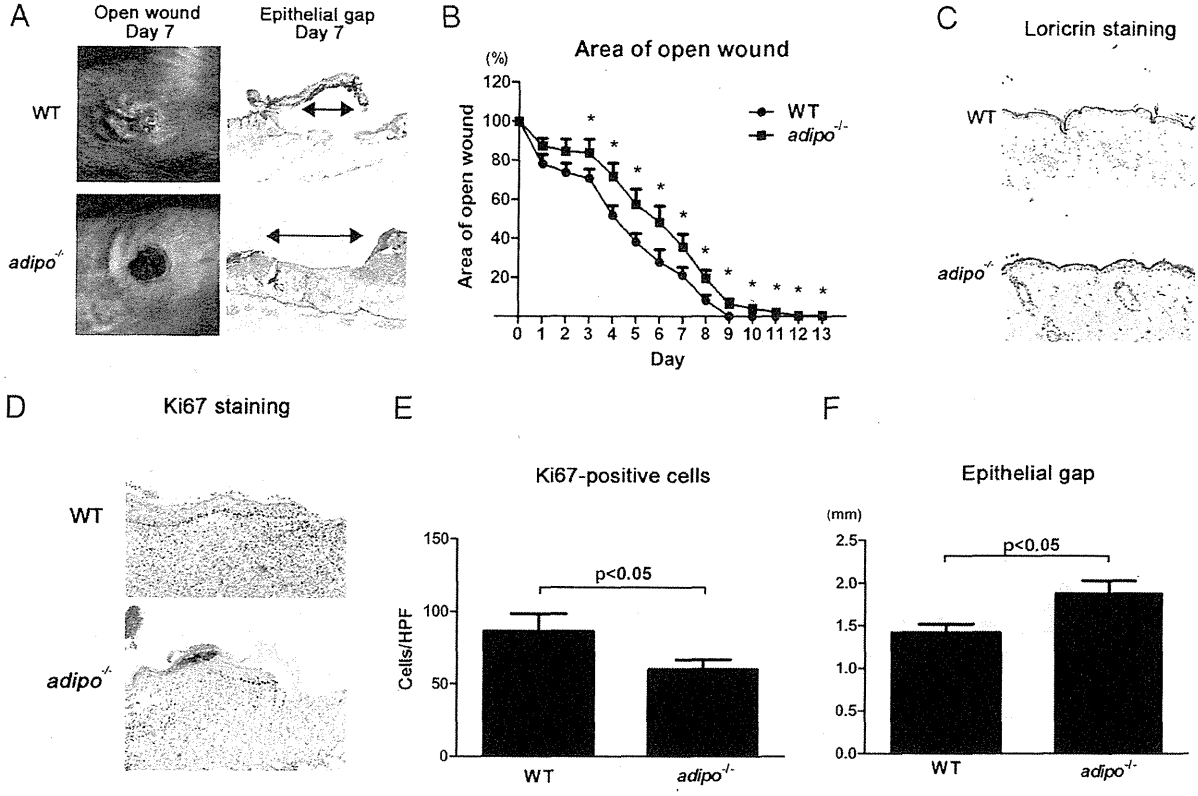

FIGURE 6. The kinetics of wound closure and evaluation of proliferative and migratory properties in adiponectin-deficient and wild-type mice. (**A**) Representative photographs of open wounds at day 7 and histology of the epithelial gap in wild-type and adiponectin-deficient mice (original magnification ×40). In histological sections, the edges of keratinocytes are indicated by arrows. (**B**) Area of open wound in wild-type and adiponectin-deficient mice was evaluated daily. Fifty wounds from 16 wild-type and 45 wounds from 14 adiponectin-deficient mice were used for the analysis. Data are shown as mean ± SE. (**C**) Immunohistochemistry of loricrin in the skin sections taken before wounding of wild-type and adiponectin-deficient mice (original magnification ×400). (**D**) Immunohistochemistry of Ki-67 in the skin sections taken 3 d after wounding of wild-type and adiponectin-deficient mice (original magnification ×200). (**E**) The number of Ki67-positive cells in keratinocytes of the wound margins 3 d after wounding. Ki67-positive cells were counted in high-power field (HPF) from 10 wounds (n = 4 mice/group). Data are shown as mean ± SE. (**F**) The epithelial gap was microscopically measured in the skin sections taken 7 d after wounding of wild-type and adiponectin-deficient mice. Thirteen wounds from six wild-type and 10 wounds from four adiponectin-deficient mice were used for the analysis. Data are shown as mean ± SE.

type and adiponectin KO mice (Fig. 7C). The expression levels of these receptors during wound repair were comparable between wild-type and adiponectin KO mice. We also analyzed AdipoR1 and AdipoR2 expression on cells in wound samples of wild-type and adiponectin KO mice by immunohistochemistry. Protein expression of AdipoR1 and AdipoR2 was detected in fibroblasts and adipocytes as well as keratinocytes, and their expression was upregulated after wounding (Fig. 7D). Taken together, adiponectin, locally produced by adipocytes after skin damage, might induce the upregulation of AdipoR1 and AdipoR2 expression on keratinocytes. This process would further enhance adiponectin-mediated signaling within keratinocytes, thus promoting keratinocyte proliferation and migration.

Systemically supplemented adiponectin ameliorates delayed wound healing in adiponectin-deficient mice but not in wild-type mice

To determine whether the impaired wound healing in adiponectin-deficient mice is particularly adiponectin dependent or not, wild-type and adiponectin-deficient mice were given daily i.p. injection of recombinant adiponectin (50 μg/day/mouse) from 1 d before wounding, and the wound repair process was examined. As shown in Fig. 8A, systemic injection of physiological dose of adiponectin significantly ameliorated impaired wound healing in adiponectin-deficient mice but not in wild-type mice at days 3 and 7. These results may indicate that adiponectin supplementation is effective only under the condition when adiponectin is insufficient.

Topically supplemented adiponectin accelerates delayed wound healing in db/db *mice but not in wild-type mice*

To evaluate a potential clinical application of adiponectin, we investigated whether adiponectin would also act directly at the wound site by administering adiponectin to wound beds directly in *db/db* mice, a rodent model for type 2 diabetes, and wild-type mice. We applied 2.5 μg adiponectin in 50 μl PBS on the left side of the murine back and the same dose of PBS on the right side under the occlusive dressing every day. *db/db* mice were previously shown to have decreased adiponectin levels and impaired wound healing (43). Topical adiponectin administration significantly reduced open wound area relative to PBS administration at days 13, 16, and 19 (Fig. 8B) in *db/db* mice. Re-epithelialization was also assessed at day 13 microscopically, and the epithelial gap was significantly shorter in adiponectin-treated mice relative to PBS-treated mice (Fig. 8C). In contrast, there was no significant difference between adiponectin- and PBS-applied wound areas in wild-type mice (Fig. 8D). These results, as in the case with systemic supplementation, suggest that wound treatment with topical adiponectin is effective in mice with low adiponectin levels (*db/db* mice) but not in mice with normal adiponectin levels (wild-type mice).